parenchymal and stromal cells in response to tissue stress or malfunction, thereby leading to functional maladaptation and tissue remodeling [12]. Recent studies have demonstrated that obese adipose tissue is characterized by adipocyte hypertrophy, followed by increased angiogenesis, immune cell infiltration, extracellular matrix overproduction, and thus, increased production of proinflammatory adipocytokines during the progression of chronic inflammation (**Fig. 1**) [1, 2, 13, 14]. This is reminiscent of the chronic inflammatory responses in atherosclerotic vascular walls, termed vascular remodeling, which is mediated through complex interactions among vascular endothelial cells, vascular smooth muscle cells, lymphocytes, and monocyte-derived macrophages (Fig. 1) [4]. Thus, the dynamic change seen in obese adipose tissue can be referred to as adipose tissue remodeling, in which stromal cells change dramatically in number and cell type during the course of obesity (Fig. 1). Given the multifunctional roles in a variety of biological contexts, among stromal cells, macrophages should play a central role in adipose tissue remodeling. In this regard, adipose tissue remodeling may be viewed as chronic inflammation that involves adipocyte hypertrophy, macrophage infiltration, and adipocyte-macrophage interaction (**Fig. 2**).

ADIPOSE TISSUE MACROPHAGE INFILTRATION

A previous study with bone marrow transplantation demonstrated that most macrophages in the adipose tissue are derived from the bone marrow [7]. In this regard, increased expression of chemokines in obese adipose tissue has been implicated in the control of monocyte recruitment to the adipose tissue. There is considerable evidence for the pathophysiologic role of the MCP-1/CCR2 pathway in macrophage infiltration into obese adipose tissue {Fig. 2, (ii) [15–18]}. Weisberg et al. [15] reported the attenuation of macrophage accumulation and chronic inflammation in the adipose tissue from mice lacking CCR2 ($CCR2^{-/-}$ mice) during a high-fat diet. Moreover, two previous studies with transgenic mice overexpressing MCP-1 in the adipose tissue and MCP-1-deficient mice ($MCP\text{-}1^{-/-}$ mice) showed that MCP-1 plays a role in the recruitment of macrophages into obese adipose tissue [16, 17]. Through a combination of a real-time horizontal chemotaxis assay in vitro and bone marrow transplantation techniques in vivo, we have also demonstrated that CCR2 expressed in bone marrow cells is involved in macrophage infiltration into obese adipose tissue [18]. In addition to the MCP-1/CCR2 pathway, there are several reports suggesting the potential involvement of other chemotactic factors in obesity-induced macrophage infiltration [19, 20]. For instance, recent evidence suggested the role of osteopontin, angiopoietin-like protein 2, and CXCL14 [19–21]. Importantly, inhibition of macrophage infiltration into obese adipose tissue through genetic and/or pharmacologic strategies improved the dysregulation of adipocytokine production, thereby leading to the amelioration of obesity-induced adipose tissue inflammation and insulin resistance. Understanding the molecular mechanisms underlying increased macrophage infiltration into obese adipose tissue may lead to the identification of novel, adipocyte-derived chemokine(s) and even therapeutic strategies to prevent or treat obesity-induced adipose tissue inflammation.

ADIPOCYTE HYPERTROPHY AND INFLAMMATORY CHANGES

To understand how macrophages are recruited into obese adipose tissue, it is important to know the molecular mechanism underlying increased production of chemokines in the early stages of obesity. Recent studies have demonstrated that multiple intracellular signaling pathways are activated in adipocytes during the course of adipocyte hypertrophy in vitro and in obese adipose tissue in vivo {Fig. 2, (i) [1–3]}. For instance, MAPKs, such as ERK, p38 MAPK, and JNK, are activated in a variety of cellular processes including adipocyte differentiation and hypertrophy [22–24]. Once activated by the upstream ki-

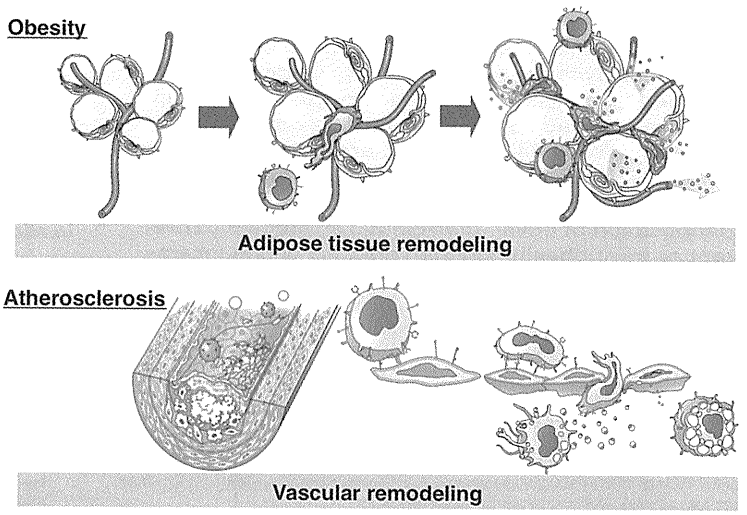

Figure 1. Adipose tissue remodeling. Obesity-induced adipose tissue inflammation is characterized by adipocyte hypertrophy, followed by increases in angiogenesis, immune cell infiltration, extracellular matrix overproduction, and thus, increased production of proinflammatory adipocytokines, which can be referred to as "adipose tissue remodeling." This is similar to chronic inflammatory changes and tissue remodeling in atherosclerotic vascular walls termed "vascular remodeling," which is mediated through complex interactions among vascular endothelial cells, vascular smooth muscle cells, lymphocytes, and monocyte-derived macrophages.

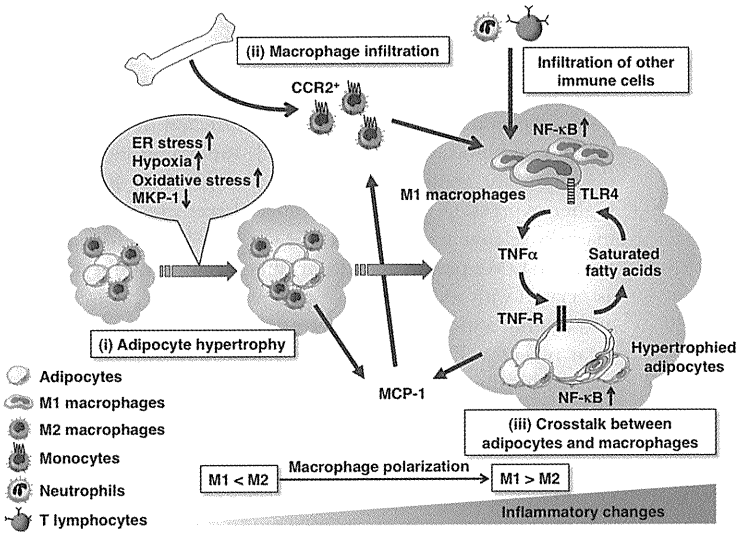

Figure 2. Molecular mechanism underlying adipose tissue inflammation. In the early stages of obesity, adipocytes should be hypertrophied in response to overnutrition (i). Recent evidence suggests that increased metabolic stresses such as ER stress, hypoxia, and oxidative stress and down-regulation of MKP-1 are involved in the induction of inflammatory changes in adipocytes during the course of adipocyte hypertrophy. In the advanced stages of obesity, there are various kinds of stromal immune cells such as neutrophils, T lymphocytes, and macrophages, which infiltrate into obese adipose tissue (ii) and thus, enhance the inflammatory changes through the crosstalk with parenchymal adipocytes (iii). For example, the macrophage-derived TNF-α induces the release of saturated fatty acids from adipocytes via lipolysis, which in turn, induces inflammatory changes in macrophages via TLR4. Such a paracrine loop between adipocytes and macrophages constitutes a vicious cycle, thereby accelerating further adipose tissue inflammation. Recent evidence has also pointed to the heterogeneity of adipose tissue macrophages; i.e., M1 or "classically activated" (proinflammatory) macrophages and M2 or "alternatively activated" (anti-inflammatory) macrophages. Infiltrated macrophages exhibit a phenotypic change from M2 to M1 polarization in obese adipose tissue, thereby accelerating adipose tissue inflammation. TNF-R, TNF-α receptor.

nases, e.g., MEK, MAPKs are inactivated rapidly by a family of protein phosphatases such as MKP-1, an inducible dual-specificity phosphatase [25, 26]. We have demonstrated that down-regulation of MKP-1 is critical for increased production of MCP-1 during the course of adipocyte hypertrophy [27]. On the other hand, Ozcan et al. [28] reported that obesity is associated with the induction of ER stress, predominantly in the adipose tissue and liver, and suggested that ER stress plays a critical role in obesity-induced adipose tissue inflammation. In this regard, Hosogai et al. [29] reported hypoxia-induced ER stress in obese adipose tissue, which is involved in the dysregulation of adipocytokine production. Moreover, Furukawa et al. [30] also showed that reactive oxygen species production is increased in parallel with adipocyte hypertrophy and that oxidative stress induces the dysregulation of adipocytokine production. It is interesting to investigate how such multiple intracellular signaling pathways are integrated during the course of adipocyte hypertrophy and/or in the early stages of obesity.

PARACRINE LOOP BETWEEN ADIPOCTYES AND MACROPHAGES

Once infiltrated into the adipose tissue in the advanced stages of obesity, macrophages participate in the inflammatory pathways that are activated in obese adipose tissue [1, 2]. Using an in vitro coculture system composed of adipocytes and macrophages, we have demonstrated that a paracrine loop involving saturated fatty acids and TNF-α derived from adipocytes and macrophages, respectively, establishes a vicious cycle that augments the inflammatory changes; i.e., marked up-regulation of proinflammatory adipocytokines, such as MCP-1 and TNF-α, and significant down-regulation of anti-inflammatory adiponectin {Fig. 2, (iii) [31]}. As the coculture-induced dysregulation of adipocytokine production is roughly parallel to that in obese adipose tissue in vivo, there may be an intimate crosstalk between adipocytes and macrophages as a potential mechanism that aggravates chronic inflammation in obese adipose tissue. Indeed, TNF-α, which is derived mostly from infiltrated macrophages in obese adipose tissue, acts on TNF-α receptor in hypertrophied adipocytes, thereby inducing proinflammatory cytokine production and adipocyte lipolysis via NF-κB-dependent and -independent (possibly MAPK-dependent) mechanisms, respectively [31]. On the other hand, saturated fatty acids thus released serve as a naturally occurring ligand for the TLR4 complex, which is essential for the recognition of LPS to induce NF-κB activation in macrophages [32, 33].

Evidence has accumulated, suggesting that TLR4 plays an important role in obesity-induced adipose tissue inflammation and systemic glucose and lipid metabolism in vivo [34–37]. As TLR4 is expressed in macrophages more abundantly than in adipocytes, it is likely that chronic inflammatory responses induced by the interaction between adipocytes and macrophages are largely mediated via TLR4 in macrophages. This discussion is supported by a recent report by Saberi et al. [38] showing that hematopoietic cell-specific deletion of TLR4 ameliorates high-fat, diet-induced hepatic and adipose tissue insulin resistance. It is, therefore, likely that inhibition of macrophages activated by adipocyte-derived saturated fatty acids may offer a unique, therapeutic strategy to prevent obesity-induced adipose tissue inflammation. Given the antagonistic relationship between saturated and *n-3* polyunsaturated fatty acids such as EPA [39], we have provided evidence that highly purified EPA increases the otherwise reduced secretion of anti-inflammatory adiponectin in obese adipose tissue, at least partly by interrupting the vicious cycle created by adipocytes and macrophages [40].

The dysregulation of adipocytokine production, which is induced by adipose tissue inflammation, may play a critical

role in the pathophysiology of the metabolic syndrome and atherosclerosis [1–4]. For instance, TNF-α, which is derived mostly from macrophages, is increased in obese adipose tissue [7, 8], and TNF-α-deficient mice are protected from obesity-induced insulin resistance [41]. By contrast, adiponectin, which is expressed exclusively in adipocytes, is markedly down-regulated in obese adipose tissue [42, 43], and supplementation of adiponectin in obese mice effectively reverses insulin resistance in the skeletal muscle and liver [42, 43]. On the other hand, MCP-1 is derived from adipocytes and macrophages in obese adipose tissue [7, 8]. Overproduction of MCP-1 in obese adipose tissue induces macrophage infiltration into the adipose tissue, thereby aggravating adipose tissue inflammation [16, 17]. It also induces insulin resistance directly in the skeletal muscle and liver, suggesting a role as an endocrine hormone [17, 44]. Finally, adipocyte-derived leptin acts directly on the hypothalamus, where it regulates food intake and energy expenditure [45, 46]. Several previous reports demonstrated that vascular remodeling and tissue fibrosis are markedly attenuated in leptin-deficient *ob/ob* mice or leptin signaling-deficient *db/db* mice [47–49]. However, the role of leptin in adipose tissue inflammation still remains to be elucidated.

PHENOTYPIC CHANGE OF ADIPOSE TISSUE MACROPHAGES

Recent studies have pointed to the heterogeneity of macrophages infiltrated into obese adipose tissue; i.e., they follow at least two different polarization states: M1 or classically activated (proinflammatory) macrophages, which are induced by proinflammatory mediators such as LPS and Th1 cytokine IFN-γ, and M2 or alternatively activated (anti-inflammatory) macrophages, which are generated in vitro by exposure to Th2 cytokines such as IL-4 and IL-13 [50, 51]. Evidence has accumulated indicating that macrophages exhibit the phenotypic change from M2 to M1 polarization in obese adipose tissue, thereby accelerating adipose tissue inflammation (Fig. 2) [50–54]. Like LPS, saturated fatty acids, as an endogenous ligand for the TLR4 complex, may contribute to the polarization of infiltrated macrophages toward M1 during the interaction between adipocytes and macrophages.

Through a combination of cDNA microarray analysis of saturated fatty acid-stimulated macrophages in vitro and obese adipose tissue in vivo, we have identified recently ATF3, a member of the ATF/CREB family of basic leucine zipper-type transcription factors, as a target gene of saturated fatty acids/TLR4 signaling in macrophages in obese adipose tissue [55]. Transgenic overexpression of ATF3 in macrophages does not affect adipocyte hypertrophy and macrophage infiltration in obese adipose tissue in vivo [55]. Interestingly, mRNA expression of M1 macrophage markers such as CD11c and TNF-α in macrophage-specific ATF3 transgenic mice is reduced significantly relative to wild-type mice, although there is no significant difference in mRNA expression of M2 macrophage markers (mannose receptor and arginase 1) between the genotypes [55]. These findings, taken together, suggest that ATF3 acts as a transcriptional repressor of saturated fatty acids/TLR4 signaling in macrophages, thereby representing a negative-feedback mechanism that attenuates obesity-induced macrophage activation in obese adipose tissue.

Prior to macrophage infiltration at the site of chronic inflammation, M1 and M2 markers are detected in circulating peripheral blood monocytes [56, 57]. Indeed, monocytes in obese and/or obese type 2 diabetic patients show significantly higher expression of M1 markers and lower expression of M2 markers relative to normal-weight controls [56]. The unbalanced M1/M2 phenotype of peripheral blood monocytes is associated with impairment of several metabolic parameters and arterial stiffness [56]. Interestingly, activation of the nuclear receptor, PPARγ by pioglitazone, a thiazolidinedione class of insulin sensitizer, improves the unbalanced M1/M2 phenotype of monocytes [56, 57], which may contribute to its antidiabetic and antiatherogenic effect. The above discussion is consistent with recent observations that PPARγ and PPARδ can stimulate M2 polarization of adipose tissue macrophages and thus, systemic insulin sensitivity [52–54, 58]. On the other hand, pioglitazone treatment improves the unbalanced M1/M2 phenotype of adipose tissue macrophages in diet-induced obese mice [59]. Moreover, a recent study suggests that macrophage PPARγ is required for full antidiabetic effects of thiazolidinediones [60]. Collectively, phenotypic modulation of adipose tissue macrophages may offer a novel, therapeutic strategy to treat or prevent the progression of obesity-induced complications such as diabetes and atherosclerosis.

OTHER IMMUNE CELLS

In addition to macrophages, other immune cells, such as neutrophils and NK cells, are increased in the adipose tissue during the course of obesity (Fig. 2) [61, 62]. Similar to the sequence of events that comprises acute inflammation, a transient increase in neutrophil infiltration precedes macrophage infiltration in a mouse model of diet-induced obesity [62], suggesting the role of neutrophils in the initiation of the inflammatory cascade. Recent evidence has also revealed a large number of T lymphocytes in the adipose tissue from lean and obese mice [63–66]. For instance, the population of $CD8^+$ T cells in the SVF is increased significantly early in the onset of obesity and continues to increase thereafter [63]. Of note, the increase in $CD8^+$ T cells precedes the accumulation of adipose tissue macrophages [63], suggesting the role of $CD8^+$ T cells in the initiation of adipose tissue inflammation. By contrast, the population of $CD4^+$ T cells and regulatory T cells is decreased in the advanced stages of obesity [63–65]. Such imbalance of the T cell subpopulation may play a role in the progression of obesity-induced adipose tissue inflammation. On the other hand, Moro et al. [67] have reported recently a new type of lymphocytes, "natural helper cells" in a novel lymphoid structure associated with adipose tissues in the peritoneal cavity. They also showed that the novel, innate lymphocytes are capable of producing large amounts of Th2 cytokines [67]. It would be interesting to elucidate the physiologic and pathophysiologic role of natural helper cells in visceral fat obesity.

ADIPOSE TISSUE INFLAMMATION AS "HOMEOSTATIC INFLAMMATION"

In addition to exogenous pathogens such as bacteria and viruses, the immune system is capable of sensing endogenous ligands released from damaged and stressed cells and tissues, thereby inducing sterile inflammation (**Fig. 3**) [12, 68, 69]. The endogenous stress signals, which are called DAMPs or "danger signals," include HMGB1, S100A8, and S100A9, modified low-density lipoproteins, and degradation products of extracellular matrices [12, 68, 69]. The danger signals, which are derived from parenchymal cells, are recognized by immune cells such as macrophages through pathogen sensors or PRRs such as TLRs, nucleotide-binding oligomerization domain-like receptors, retinoid-inducible gene-like receptors, scavenger receptors, and C-type lectin receptors [12, 68, 69].

A previous study showed that macrophages in obese adipose tissue are localized to dead adipocytes, where they fuse to scavenge the residual lipid droplet and ultimately, form multinucleate giant cells, a hallmark of chronic inflammation [70]. Indeed, macrophages aggregate to constitute a CLS surrounding dead adipocytes in advanced obesity [13, 14, 70]. Electron microscopic analysis also revealed lipid-laden phagolysosomes in macrophages within CLS [70]. Given that TNF-α induces proapoptotic and/or death signals in a variety of cell types, it is therefore interesting to speculate that hypertrophied adipocytes, which are stimulated and thus, dying by macrophage-derived TNF-α, can release saturated fatty acids as an endogenous danger signal that report their diseased state to macrophages in obese adipose tissue. Indeed, several lines of evidence indicate that adipocyte death and/or the death receptor Fas signaling contribute to obesity-induced adipose tissue inflammation and systemic insulin resistance [71, 72]. On the other hand, free fatty acids are an important energy source mobilized from triglycerides stored in the adipose tissue, particularly during periods of starvation, but recent evidence has suggested the pathophysiologic roles other than the supply of nutrients in times of fasting or increased energy demand. In this regard, free fatty acids, when released physiologically during fasting or starvation via adipocyte lipolysis, may not act as a danger signal. Similar to the relationship between commensal bacteria and pathogen sensors in epithelial cell homeostasis within the intestinal mucosa, activation of the TLR4 complex by saturated fatty acids may be involved in the regulation of metabolic homeostasis within the adipose tissue (Fig. 3). Sustained interaction between endogenous ligands, which are derived from parenchymal cells and pathogen sensors, expressed in stromal immune cells, should lead to chronic/homeostatic inflammatory responses ranging from the basal homeostatic state to diseased tissue remodeling, which may be referred to as homeostatic inflammation (Fig. 3). Dysregulation of this process can result in a variety of chronic inflammatory diseases, such as obesity, diabetes mellitus, atherosclerosis, malignant cancers, autoimmune diseases, and even neurodegenerative diseases. Collectively, adipose tissue inflammation may represent a prototypic example of homeostatic inflammation.

CONCLUDING REMARKS

The adipose tissue communicates with multiple organs or tissues by virtue of a large number of adipocytokines and thus, influences a variety of physiologic and pathophysiologic processes. Obesity may be viewed as a chronic, low-grade inflammatory as well as a metabolic disease; chronic inflammation within the adipose tissue or adipose tissue remodeling results in the dysregulation of adipocytokine production, thereby contributing to the pathophysiology of the metabolic syndrome. Among stromal cells, macrophages should play a critical role in obesity-related adipose tissue inflammation. During the paracrine interaction between adipocytes and macrophages, saturated fatty acids, which are released from hypertrophied

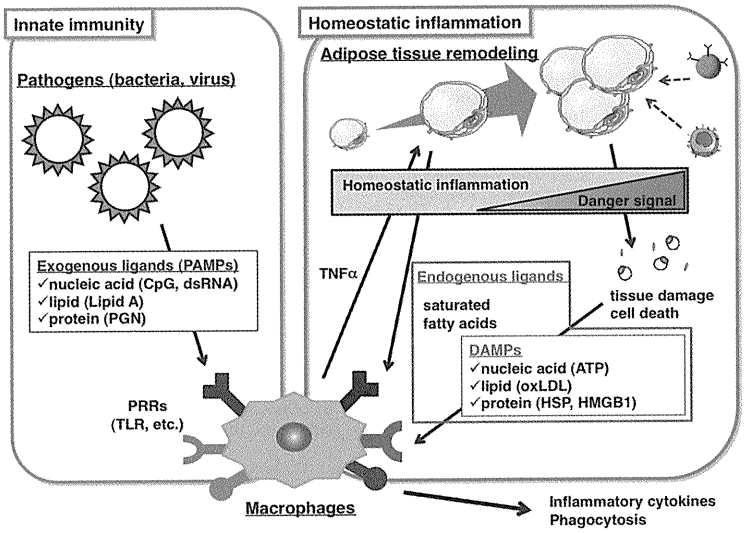

Figure 3. Adipose tissue inflammation as homeostatic inflammation. In "innate immunity," exogenous ligands (PAMPs) are sensed by PRRs, thereby inducing inflammatory changes. On the other hand, DAMPs, released from damaged or stressed cells and tissues, can activate PRRs, thereby inducing homeostatic inflammation ranging from the basal homeostatic state to diseased tissue remodeling. The role of endogenous ligands as a danger signal has been emphasized during the progression of homeostatic inflammation. For instance, free fatty acids, when released as an energy source during fasting or starvation, may not act as a danger signal. However, in adipose tissue inflammation, saturated fatty acids, which are released from hypertrophied adipocytes, can report, as a danger signal, their diseased state to macrophages via the TLR4 complex during the course of obesity. dsRNA, Double-stranded RNA; PGN, peptidoglycan; ATP, adenosine triphosphate; oxLDL, oxidized low-density lipoprotein; HSP, heat shock protein.

adipocytes via the macrophage-induced lipolysis, serve as an endogenous ligand for the TLR4 complex, a major pathogen sensor, to activate macrophages for the regulation of metabolic homeostasis, which is a hallmark of homeostatic inflammation. Understanding the molecular mechanism underlying homeostatic inflammation of obese adipose tissue may lead to novel, therapeutic strategies to prevent or treat obesity-induced adipose tissue inflammation.

ACKNOWLEDGMENTS

Work in the authors' laboratory was supported in part by a grant-in-aid for scientific research from the Ministry of Education, Culture, Sports, Science and Technology of Japan and the Ministry of Health, Labor and Welfare of Japan. We thank Dr. Kensuke Miyake (The Institute of Medical Science, University of Tokyo) for discussions.

REFERENCES

1. Schenk, S., Saberi, M., Olefsky, J. M. (2008) Insulin sensitivity: modulation by nutrients and inflammation. *J. Clin. Invest.* **118,** 2992–3002.
2. Hotamisligil, G. S. (2006) Inflammation and metabolic disorders. *Nature* **444,** 860–867.
3. Berg, A. H., Scherer, P. E. (2005) Adipose tissue, inflammation, and cardiovascular disease. *Circ. Res.* **96,** 939–949.
4. Rocha, V. Z., Libby, P. (2009) Obesity, inflammation, and atherosclerosis. *Nat. Rev. Cardiol.* **6,** 399–409.
5. Matsuzawa, Y., Funahashi, T., Nakamura, T. (1999) Molecular mechanism of metabolic syndrome X: contribution of adipocytokines adipocyte-derived bioactive substances. *Ann. N. Y. Acad. Sci.* **892,** 146–154.
6. Kadowaki, T., Yamauchi, T., Kubota, N., Hara, K., Ueki, K., Tobe, K. (2006) Adiponectin and adiponectin receptors in insulin resistance, diabetes, and the metabolic syndrome. *J. Clin. Invest.* **116,** 1784–1792.
7. Weisberg, S. P., McCann, D., Desai, M., Rosenbaum, M., Leibel, R. L., Ferrante Jr., A. W. (2003) Obesity is associated with macrophage accumulation in adipose tissue. *J. Clin. Invest.* **112,** 1796–1808.
8. Xu, H., Barnes, G. T., Yang, Q., Tan, G., Yang, D., Chou, C. J., Sole, J., Nichols, A., Ross, J. S., Tartaglia, L. A., Chen, H. (2003) Chronic inflammation in fat plays a crucial role in the development of obesity-related insulin resistance. *J. Clin. Invest.* **112,** 1821–1830.
9. Clement, K., Viguerie, N., Poitou, C., Carette, C., Pelloux, V., Curat, C. A., Sicard, A., Rome, S., Benis, A., Zucker, J. D., Vidal, H., Laville, M., Barsh, G. S., Basdevant, A., Stich, V., Cancello, R., Langin, D. (2004) Weight loss regulates inflammation-related genes in white adipose tissue of obese subjects. *FASEB J.* **18,** 1657–1669.
10. Wasserman, F. (1965) *Handbook of Physiology.* Washington, DC, USA, American Physiology Society.
11. Serhan, C. N., Savill, J. (2005) Resolution of inflammation: the beginning programs the end. *Nat. Immunol.* **6,** 1191–1197.
12. Medzhitov, R. (2008) Origin and physiological roles of inflammation. *Nature* **454,** 428–435.
13. Nishimura, S., Manabe, I., Nagasaki, M., Hosoya, Y., Yamashita, H., Fujita, H., Ohsugi, M., Tobe, K., Kadowaki, T., Nagai, R., Sigiura, S. (2007) Adipogenesis in obesity requires close interplay between differentiating adipocytes, stromal cells, and blood vessels. *Diabetes* **56,** 1517–1526.
14. Nishimura, S., Manabe, I., Nagasaki, M., Seo, K., Yamashita, H., Hosoya, Y., Ohsugi, M., Tobe, K., Kadowaki, T., Nagai, R., Sigiura, S. (2008) In vivo imaging in mice reveals local cell dynamics and inflammation in obese adipose tissue. *J. Clin. Invest.* **118,** 710–721.
15. Weisberg, S. P., Hunter, D., Huber, R., Lemieux, J., Slaymaker, S., Vaddi, K., Charo, I., Leibel, R. L., Ferrante Jr., A. W. (2006) CCR2 modulates inflammatory and metabolic effects of high-fat feeding. *J. Clin. Invest.* **116,** 115–124.
16. Kanda, H., Tateya, S., Tamori, Y., Kotani, K., Hiasa, K., Kitazawa, R., Kitazawa, S., Miyachi, H., Maeda, S., Egashira, K., Kasuga, M. (2006) MCP-1 contributes to macrophage infiltration into adipose tissue, insulin resistance, and hepatic steatosis in obesity. *J. Clin. Invest.* **116,** 1494–1505.
17. Kamei, N., Tobe, K., Suzuki, R., Ohsugi, M., Watanabe, T., Kubota, N., Ohtsuka-Kowatari, N., Kumagai, K., Sakamoto, K., Kobayashi, M., Yamauchi, T., Ueki, K., Oishi, Y., Nishimura, S., Manabe, I., Hashimoto, H., Ohnishi, Y., Ogata, H., Tokuyama, K., Tsunoda, M., Ide, T., Murakami, K., Nagai, R., Kadowaki, T. (2006) Overexpression of monocyte chemoattractant protein-1 in adipose tissues causes macrophage recruitment and insulin resistance. *J. Biol. Chem.* **281,** 26602–26614.
18. Ito, A., Suganami, T., Yamauchi, A., Degawa-Yamauchi, M., Tanaka, M., Kouyama, R., Kobayashi, Y., Nitta, N., Yasuda, K., Hirata, Y., Kuziel, W. A., Takeya, M., Kanegasaki, S., Kamei, Y., Ogawa, Y. (2008) Role of CC chemokine receptor 2 in bone marrow cells in the recruitment of macrophages into obese adipose tissue. *J. Biol. Chem.* **283,** 35715–35723.
19. Nomiyama, T., Perez-Tilve, D., Ogawa, D., Gizard, F., Zhao, Y., Heywood, E. B., Jones, K. L., Kawamori, R., Cassis, L. A., Tschop, M. H., Bruemmer, D. (2007) Osteopontin mediates obesity-induced adipose tissue macrophage infiltration and insulin resistance in mice. *J. Clin. Invest.* **117,** 2877–2888.
20. Nara, N., Nakayama, Y., Okamoto, S., Tamura, H., Kiyono, M., Muraoka, M., Tanaka, K., Taya, C., Shitara, H., Ishii, R., Yonekawa, H., Minokoshi, Y., Hara, T. (2007) Disruption of CXC motif chemokine ligand-14 in mice ameliorates obesity-induced insulin resistance. *J. Biol. Chem.* **282,** 30794–30803.
21. Tabata, M., Kadomatsu, T., Fukuhara, S., Miyata, K., Ito, Y., Endo, M., Urano, T., Zhu, H. J., Tsukano, H., Tazume, H., Kaikita, K., Miyashita, K., Iwawaki, T., Shimabukuro, M., Sakaguchi, K., Ito, T., Nakagata, N., Yamada, T., Katagiri, H., Kasuga, M., Ando, Y., Ogawa, H., Mochizuki, N., Itoh, H., Suda, T., Oike, Y. (2009) Angiopoietin-like protein 2 promotes chronic adipose tissue inflammation and obesity-related systemic insulin resistance. *Cell Metab.* **10,** 178–188.
22. Johnson, G. L., Lapadat, R. (2002) Mitogen-activated protein kinase pathways mediated by ERK, JNK, and p38 protein kinases. *Science* **298,** 1911–1912.
23. Bost, F., Aouadi, M., Caron, L., Binetruy, B. (2005) The role of MAPKs in adipocyte differentiation and obesity. *Biochimie* **87,** 51–56.
24. Hirosumi, J., Tuncman, G., Chang, L., Gorgun, C. Z., Uysal, K. T., Maeda, K., Karin, M., Hotamisligil, G. S. (2002) A central role for JNK in obesity and insulin resistance. *Nature* **420,** 333–336.
25. Farooq, A., Zhou, M. M. (2004) Structure and regulation of MAPK phosphatases. *Cell. Signal.* **16,** 769–779.
26. Keyse, S. M. (2000) Protein phosphatases and the regulation of mitogen-activated protein kinase signaling. *Curr. Opin. Cell Biol.* **12,** 186–192.
27. Ito, A., Suganami, T., Miyamoto, Y., Yoshimasa, Y., Takeya, M., Kamei, Y., Ogawa, Y. (2007) Role of MAPK phosphatase-1 in the induction of monocyte chemoattractant protein-1 during the course of adipocyte hypertrophy. *J. Biol. Chem.* **282,** 25445–25452.
28. Ozcan, U., Cao, Q., Yilmaz, E., Lee, A. H., Iwakoshi, N. N., Ozdelen, E., Tuncman, G., Gorgun, C., Glimcher, L. H., Hotamisligil, G. S. (2004) Endoplasmic reticulum stress links obesity, insulin action, and type 2 diabetes. *Science* **306,** 457–461.
29. Hosogai, N., Fukuhara, A., Oshima, K., Miyata, Y., Tanaka, S., Segawa, K., Furukawa, S., Tochino, Y., Komuro, R., Matsuda, M., Shimomura, I. (2007) Adipose tissue hypoxia in obesity and its impact on adipocytokine dysregulation. *Diabetes* **56,** 901–911.
30. Furukawa, S., Fujita, T., Shimabukuro, M., Iwaki, M., Yamada, Y., Nakajima, Y., Nakayama, O., Makishima, M., Matsuda, M., Shimomura, I. (2004) Increased oxidative stress in obesity and its impact on metabolic syndrome. *J. Clin. Invest.* **114,** 1752–1761.
31. Suganami, T., Nishida, J., Ogawa, Y. (2005) A paracrine loop between adipocytes and macrophages aggravates inflammatory changes: role of free fatty acids and tumor necrosis factor α. *Arterioscler. Thromb. Vasc. Biol.* **25,** 2062–2068.
32. Suganami, T., Tanimoto-Koyama, K., Nishida, J., Itoh, M., Yuan, X., Mizuarai, S., Kotani, H., Yamaoka, S., Miyake, K., Aoe, S., Kamei, Y., Ogawa, Y. (2007) Role of the Toll-like receptor 4/NF-κB pathway in saturated fatty acid-induced inflammatory changes in the interaction between adipocytes and macrophages. *Arterioscler. Thromb. Vasc. Biol.* **27,** 84–91.
33. Lee, J. Y., Sohn, K. H., Rhee, S. H., Hwang, D. (2001) Saturated fatty acids, but not unsaturated fatty acids, induce the expression of cyclooxygenase-2 mediated through Toll-like receptor 4. *J. Biol. Chem.* **276,** 16683–16689.
34. Suganami, T., Mieda, T., Itoh, M., Shimoda, Y., Kamei, Y., Ogawa, Y. (2007) Attenuation of obesity-induced adipose tissue inflammation in C3H/HeJ mice carrying a Toll-like receptor 4 mutation. *Biochem. Biophys. Res. Commun.* **354,** 45–49.
35. Shi, L., Kishore, R., McMullen, M. R., Nagy, L. E. (2002) Lipopolysaccharide stimulation of ERK1/2 increases TNF-α production via Egr-1. *Am. J. Physiol. Cell Physiol.* **282,** C1205–C1211.
36. Poggi, M., Bastelica, D., Gual, P., Iglesias, M. A., Gremeaux, T., Knauf, C., Peiretti, F., Verdier, M., Juhan-Vague, I., Tanti, J. F., Burcelin, R., Alessi, M. C. (2007) C3H/HeJ mice carrying a Toll-like receptor 4 mutation are protected against the development of insulin resistance in white adipose tissue in response to a high-fat diet. *Diabetologia* **50,** 1267–1276.
37. Tsukumo, D. M., Carvalho-Filho, M. A., Carvalheira, J. B., Prada, P. O., Hirabara, S. M., Schenka, A. A., Araujo, E. P., Vassallo, J., Curi, R., Velloso, L. A., Saad, M. J. (2007) Loss-of-function mutation in Toll-like receptor 4 prevents diet-induced obesity and insulin resistance. *Diabetes* **56,** 1986–1998.
38. Saberi, M., Woods, N. B., de Luca, C., Schenk, S., Lu, J. C., Bandyopadhyay, G., Verma, I. M., Olefsky, J. M. (2009) Hematopoietic cell-specific deletion of Toll-like receptor 4 ameliorates hepatic and adipose tissue insulin resistance in high-fat-fed mice. *Cell Metab.* **10,** 419–429.

39. Lee, J. Y., Plakidas, A., Lee, W. H., Heikkinen, A., Chanmugam, P., Bray, G., Hwang, D. H. (2003) Differential modulation of Toll-like receptors by fatty acids: preferential inhibition by n-3 polyunsaturated fatty acids. *J. Lipid Res.* **44,** 479–486.
40. Itoh, M., Suganami, T., Satoh, N., Tanimoto-Koyama, K., Yuan, X., Tanaka, M., Kawano, H., Yano, T., Aoe, S., Takeya, M., Shimatsu, A., Kuzuya, H., Kamei, Y., Ogawa, Y. (2007) Increased adiponectin secretion by highly purified eicosapentaenoic acid in rodent models of obesity and human obese subjects. *Arterioscler. Thromb. Vasc. Biol.* **27,** 1918–1925.
41. Uysal, K. T., Wiesbrock, S. M., Marino, M. W., Hotamisligil, G. S. (1997) Protection from obesity-induced insulin resistance in mice lacking TNF-α function. *Nature* **389,** 610–614.
42. Yamauchi, T., Kamon, J., Waki, H., Terauchi, Y., Kubota, N., Hara, K., Mori, Y., Ide, T., Murakami, K., Tsuboyama-Kasaoka, N., Ezaki, O., Akanuma, Y., Gavrilova, O., Vinson, C., Reitman, M. L., Kagechika, H., Shudo, K., Yoda, M., Nakano, Y., Tobe, K., Nagai, R., Kimura, S., Tomita, M., Froguel, P., Kadowaki, T. (2001) The fat-derived hormone adiponectin reverses insulin resistance associated with both lipoatrophy and obesity. *Nat. Med.* **7,** 941–946.
43. Maeda, N., Shimomura, I., Kishida, K., Nishizawa, H., Matsuda, M., Nagaretani, H., Furuyama, N., Kondo, H., Takahashi, M., Arita, Y., Komuro, R., Ouchi, N., Kihara, S., Tochino, Y., Okutomi, K., Horie, M., Takeda, S., Aoyama, T., Funahashi, T., Matsuzawa, Y. (2002) Diet-induced insulin resistance in mice lacking adiponectin/ACRP30. *Nat. Med.* **8,** 731–737.
44. Tateya, S., Tamori, Y., Kawaguchi, T., Kanda, H., Kasuga, M. (2010) An increase in the circulating concentration of monocyte chemoattractant protein-1 elicits systemic insulin resistance irrespective of adipose tissue inflammation in mice. *Endocrinology* **151,** 971–979.
45. Ogawa, Y., Masuzaki, H., Hosoda, K., Aizawa-Abe, M., Suga, J., Suda, M., Ebihara, K., Iwai, H., Matsuoka, N., Satoh, N., Odaka, H., Kasuga, H., Fujisawa, Y., Inoue, G., Nishimura, H., Yoshimasa, Y., Nakao, K. (1999) Increased glucose metabolism and insulin sensitivity in transgenic skinny mice overexpressing leptin. *Diabetes* **48,** 1822–1829.
46. Friedman, J. M., Halaas, J. L. (1998) Leptin and the regulation of body weight in mammals. *Nature* **395,** 763–770.
47. Tanaka, M., Suganami, T., Sugita, S., Shimoda, Y., Kasahara, M., Aoe, S., Takeya, M., Takeda, S., Kamei, Y., Ogawa, Y. (2010) Role of central leptin signaling in renal macrophage infiltration. *Endocr. J.* **57,** 61–72.
48. Schafer, K., Halle, M., Goeschen, C., Dellas, C., Pynn, M., Loskutoff, D. J., Konstantinides, S. (2004) Leptin promotes vascular remodeling and neointimal growth in mice. *Arterioscler. Thromb. Vasc. Biol.* **24,** 112–117.
49. Stephenson, K., Tunstead, J., Tsai, A., Gordon, R., Henderson, S., Dansky, H. M. (2003) Neointimal formation after endovascular arterial injury is markedly attenuated in *db/db* mice. *Arterioscler. Thromb. Vasc. Biol.* **23,** 2027–2033.
50. Lumeng, C. N., Bodzin, J. L., Saltiel, A. R. (2007) Obesity induces a phenotypic switch in adipose tissue macrophage polarization. *J. Clin. Invest.* **117,** 175–184.
51. Lumeng, C. N., DelProposto, J. B., Westcott, D. J., Saltiel, A. R. (2008) Phenotypic switching of adipose tissue macrophages with obesity is generated by spatiotemporal differences in macrophage subtypes. *Diabetes* **57,** 3239–3246.
52. Odegaard, J. I., Ricardo-Gonzalez, R. R., Red Eagle, A., Vats, D., Morel, C. R., Goforth, M. H., Subramanian, V., Mukundan, L., Ferrante, A. W., Chawla, A. (2008) Alternative M2 activation of Kupffer cells by PPARδ ameliorates obesity-induced insulin resistance. *Cell Metab.* **7,** 496–507.
53. Odegaard, J. I., Ricardo-Gonzalez, R. R., Goforth, M. H., Morel, C. R., Subramanian, V., Mukundan, L., Red Eagle, A., Vats, D., Brombacher, F., Ferrante, A. W., Chawla, A. (2007) Macrophage-specific PPARγ controls alternative activation and improves insulin resistance. *Nature* **447,** 1116–1120.
54. Kang, K., Reilly, S. M., Karabacak, V., Gangl, M. R., Fitzgerald, K., Hatano, B., Lee, C. H. (2008) Adipocyte-derived Th2 cytokines and myeloid PPARδ regulate macrophage polarization and insulin sensitivity. *Cell Metab.* **7,** 485–495.
55. Suganami, T., Yuan, X., Shimoda, Y., Uchio-Yamada, K., Nakagawa, N., Shirakawa, I., Usami, T., Tsukahara, T., Nakayama, K., Miyamoto, Y., Yasuda, K., Matsuda, J., Kamei, Y., Kitajima, S., Ogawa, Y. (2009) Activating transcription factor 3 constitutes a negative feedback mechanism that attenuates saturated fatty acid/Toll-like receptor 4 signaling and macrophage activation in obese adipose tissue. *Circ. Res.* **105,** 25–32.
56. Satoh, N., Shimatsu, A., Himeno, A., Sasaki, Y., Yamakage, H., Yamada, K., Suganami, T., Ogawa, Y. (2010) Unbalanced M1/M2 phenotype of peripheral blood monocytes in obese diabetic patients: effect of pioglitazone. *Diabetes Care* **33,** e7.
57. Bouhlel, M. A., Derudas, B., Rigamonti, E., Dievart, R., Brozek, J., Haulon, S., Zawadzki, C., Jude, B., Torpier, G., Marx, N., Staels, B., Chinetti-Gbaguidi, G. (2007) PPARγ activation primes human monocytes into alternative M2 macrophages with anti-inflammatory properties. *Cell Metab.* **6,** 137–143.
58. Vats, D., Mukundan, L., Odegaard, J. I., Zhang, L., Smith, K. L., Morel, C. R., Wagner, R. A., Greaves, D. R., Murray, P. J., Chawla, A. (2006) Oxidative metabolism and PGC-1β attenuate macrophage-mediated inflammation. *Cell Metab.* **4,** 13–24.
59. Fujisaka, S., Usui, I., Bukhari, A., Ikutani, M., Oya, T., Kanatani, Y., Tsuneyama, K., Nagai, Y., Takatsu, K., Urakaze, M., Kobayashi, M., Tobe, K. (2009) Regulatory mechanisms for adipose tissue M1 and M2 macrophages in diet-induced obese mice. *Diabetes* **58,** 2574–2582.
60. Hevener, A. L., Olefsky, J. M., Reichart, D., Nguyen, M. T., Bandyopadyhay, G., Leung, H. Y., Watt, M. J., Benner, C., Febbraio, M. A., Nguyen, A. K., Folian, B., Subramaniam, S., Gonzalez, F. J., Glass, C. K., Ricote, M. (2007) Macrophage PPARγ is required for normal skeletal muscle and hepatic insulin sensitivity and full antidiabetic effects of thiazolidinediones. *J. Clin. Invest.* **117,** 1658–1669.
61. Ohmura, K., Ishimori, N., Ohmura, Y., Tokuhara, S., Nozawa, A., Horii, S., Andoh, Y., Fujii, S., Iwabuchi, K., Onoe, K., Tsutsui, H. (2010) Natural killer T cells are involved in adipose tissues inflammation and glucose intolerance in diet-induced obese mice. *Arterioscler. Thromb. Vasc. Biol.* **30,** 193–199.
62. Elgazar-Carmon, V., Rudich, A., Hadad, N., Levy, R. (2008) Neutrophils transiently infiltrate intra-abdominal fat early in the course of high-fat feeding. *J. Lipid Res.* **49,** 1894–1903.
63. Nishimura, S., Manabe, I., Nagasaki, M., Eto, K., Yamashita, H., Ohsugi, M., Otsu, M., Hara, K., Ueki, K., Sugiura, S., Yoshimura, K., Kadowaki, T., Nagai, R. (2009) $CD8^+$ effector T cells contribute to macrophage recruitment and adipose tissue inflammation in obesity. *Nat. Med.* **15,** 914–920.
64. Winer, S., Chan, Y., Paltser, G., Truong, D., Tsui, H., Bahrami, J., Dorfman, R., Wang, Y., Zielenski, J., Mastronardi, F., Maezawa, Y., Drucker, D. J., Engleman, E., Winer, D., Dosch, H. M. (2009) Normalization of obesity-associated insulin resistance through immunotherapy. *Nat. Med.* **15,** 921–929.
65. Feuerer, M., Herrero, L., Cipolletta, D., Naaz, A., Wong, J., Nayer, A., Lee, J., Goldfine, A. B., Benoist, C., Shoelson, S., Mathis, D. (2009) Lean, but not obese, fat is enriched for a unique population of regulatory T cells that affect metabolic parameters. *Nat. Med.* **15,** 930–939.
66. Kintscher, U., Hartge, M., Hess, K., Foryst-Ludwig, A., Clemenz, M., Wabitsch, M., Fischer-Posovszky, P., Barth, T. F., Dragun, D., Skurk, T., Hauner, H., Bluher, M., Unger, T., Wolf, A. M., Knippschild, U., Hombach, V., Marx, N. (2008) T-lymphocyte infiltration in visceral adipose tissue: a primary event in adipose tissue inflammation and the development of obesity-mediated insulin resistance. *Arterioscler. Thromb. Vasc. Biol.* **28,** 1304–1310.
67. Moro, K., Yamada, T., Tanabe, M., Takeuchi, T., Ikawa, T., Kawamoto, H., Furusawa, J., Ohtani, M., Fujii, H., Koyasu, S. (2010) Innate production of Th2 cytokines by adipose tissue-associated c-Kit^+Sca-1^+ lymphoid cells. *Nature* **463,** 540–544.
68. Medzhitov, R., Janeway Jr., C. A. (2002) Decoding the patterns of self and nonself by the innate immune system. *Science* **296,** 298–300.
69. Zhang, X., Mosser, D. M. (2008) Macrophage activation by endogenous danger signals. *J. Pathol.* **214,** 161–178.
70. Cinti, S., Mitchell, G., Barbatelli, G., Murano, I., Ceresi, E., Faloia, E., Wang, S., Fortier, M., Greenberg, A. S., Obin, M. S. (2005) Adipocyte death defines macrophage localization and function in adipose tissue of obese mice and humans. *J. Lipid Res.* **46,** 2347–2355.
71. Alkhouri, N., Gornicka, A., Berk, M. P., Thapaliya, S., Dixon, L. J., Kashyap, S., Schauer, P. R., Feldstein, A. E. (2010) Adipocyte apoptosis, a link between obesity, insulin resistance, and hepatic steatosis. *J. Biol. Chem.* **285,** 3428–3438.
72. Wueest, S., Rapold, R. A., Schumann, D. M., Rytka, J. M., Schildknecht, A., Nov, O., Chervonsky, A. V., Rudich, A., Schoenle, E. J., Donath, M. Y., Konrad, D. (2010) Deletion of Fas in adipocytes relieves adipose tissue inflammation and hepatic manifestations of obesity in mice. *J. Clin. Invest.* **120,** 191–202.

KEY WORDS:
adipocytes · homeostatic inflammation · obesity · Toll-like receptor · saturated fatty acids

OBSERVATIONS

Unbalanced M1/M2 Phenotype of Peripheral Blood Monocytes in Obese Diabetic Patients

Effect of pioglitazone

The monocyte-macrophage system exists in at least two distinct phenotypes of differentiation: proinflammatory (M1) and anti-inflammatory (M2) (1,2). Macrophages, when infiltrated into obese adipose tissue, exhibit a phenotypic switch from M2 to M1 polarization, thereby contributing to obesity-induced adipose tissue inflammation and insulin resistance (1). Expression of both M1 and M2 markers is detected in circulating peripheral blood mononuclear cells as well as in atherosclerotic plaques (3). However, there have been no detailed studies on the M1/M2 phenotype of monocytes and their association with cardiovascular risks in obese subjects with type 2 diabetes. On the other hand, we demonstrated that pioglitazone, a thiazolidinedione class of insulin sensitizer, exerts an antiatherogenic effect independent of its antidiabetic effect (4). Here, we investigated the M1/M2 phenotype of peripheral blood monocytes and pulse wave velocity (PWV), an established index of arterial stiffness, and also the effect of pioglitazone in obese diabetic patients.

A total of 161 subjects (95 men and 66 women, mean age 50.4 years), including 45 normal-weight control subjects, 62 obese nondiabetic patients, and 54 obese diabetic patients with or without pioglitazone treatment for 3 months (30 mg daily), were recruited in our clinic. Peripheral blood monocytes were prepared using magnetic-assisted cell sorting and flow cytometry with anti-CD14. Expression of M1/M2 markers was analyzed by real-time quantitative PCR method and flow cytometry. The number and percentage of $CD14^+$ cells among peripheral blood monocytes from obese diabetic patients were significantly increased relative to those of control subjects ($P < 0.05$). The $CD14^+$ cells from obese nondiabetic patients showed significantly higher expression of M1 markers, tumor necrosis factor-α, and interleukin (IL)-6 and lower expression of an M2 marker, IL-10, relative to control subjects ($P < 0.01$). This is consistent with a report that peripheral blood mononuclear cells in obesity are in an inflammatory state (5). In addition, expression of IL-10 and CD163 in $CD14^+$ cells from obese diabetic patients was significantly decreased relative to that of obese nondiabetic patients ($P < 0.01$). Multivariate regression analysis showed that expression of tumor necrosis factor-α is independently associated with age and BMI and that expression of IL-6 is independently associated with BMI and LDL cholesterol ($P < 0.01$); expression of IL-10 was negatively and independently associated with diastolic blood pressure, A1C, and triglycerides, and expression of CD163 was negatively and independently associated with insulin concentration, A1C, and PWV ($P < 0.05$). Moreover, only age and CD163 were independently correlated with PWV ($P < 0.05$). Interestingly, 3-month treatment with pioglitazone significantly increased IL-10 and CD163 and decreased IL-6 ($P < 0.05$) in parallel with the improvement of fasting plasma glucose, A1C, insulin concentration, homeostasis model assessment-insulin resistance index, and PWV in obese diabetic patients. Further studies are required to elucidate more detailed characterization of monocyte subsets in obese diabetic patients and the resulting pathophysiological implication in cardiovascular diseases.

This study provides evidence that an unbalanced M1/M2 phenotype of peripheral blood monocytes is associated with metabolic disorder and arterial stiffness in obese type 2 diabetic patients. We also demonstrate that peroxisome proliferator–activated receptor-γ activation improves the unbalanced M1/M2 phenotype of monocytes in obese diabetic patients, which may contribute to its antiatherogenic effect.

NORIKO SATOH, MD, PHD[1]
AKIRA SHIMATSU, MD, PHD[1]
AKIHIRO HIMENO, MD[1,2]
YOUSUKE SASAKI, BSC[1]
HAJIME YAMAKAGE, BSC[1]
KAZUNORI YAMADA, MD, PHD[2]
TAKAYOSHI SUGANAMI, MD, PHD[3]
YOSHIHIRO OGAWA, MD, PHD[3,4]

From the [1]Clinical Research Institute for Endocrine Metabolic Diseases, National Hospital Organization, Kyoto Medical Center, Kyoto, Japan; the [2]Diabetes Center, National Hospital Organization, Kyoto Medical Center, Kyoto, Japan; the [3]Department of Molecular Medicine and Metabolism, Medical Research Institute, Tokyo Medical and Dental University, Tokyo, Japan; and the [4]Global Center of Excellence Program, International Research Center for Molecular Science in Tooth and Bone Diseases, Tokyo Medical and Dental University, Tokyo, Japan.

Corresponding author: Noriko Satoh, nsato@kyotolan.hosp.go.jp.

DOI: 10.2337/dc09-1315

Acknowledgments— This work was supported in part by a Grant-in-Aid for Scientific Research from the Ministry of Education, Culture, Sports, Science and Technology of the Japan Ministry of Health, Labor, and Welfare of Japan (to N.S. and Y.O.), the Smoking Research Foundation (to N.S.), and Takeda Science Foundation (to Y.O.).

No other potential conflicts of interest relevant to this article were reported.

References

1. Lumeng CN, Bodzin JL, Saltiel AR. Obesity induces a phenotypic switch in adipose tissue macrophage polarization. J Clin Invest 2007;117:175–184
2. Gordon S, Taylor PR. Monocyte and macrophage heterogeneity. Nat Rev Immunol 2005;5:953–964
3. Bouhlel MA, Derudas B, Rigamonti E, Dièvart R, Brozek J, Haulon S, Zawadzki C, Jude B, Torpier G, Marx N, Staels B, Chinetti-Gbaguidi G. PPARγ activation primes human monocytes into alternative M2 macrophages with anti-inflammatory properties. Cell Metab 2007;6:137–143
4. Satoh N, Ogawa Y, Usui T, Tagami T, Kono S, Uesugi H, Sugiyama H, Sugawara A, Yamada K, Shimatsu A, Kuzuya H, Nakao K. Antiatherogenic effect of pioglitazone in type 2 diabetic patients irrespective of the responsiveness to its antidiabetic effect. Diabetes Care 2003;26:2493–2499
5. Ghanim H, Aljada A, Hofmeyer D, Syed T, Mohanty P, Dandona P. Circulating mononuclear cells in the obese are in a proinflammatory state. Circulation 2004;110:1564–1571

Hepatology Research

Hepatology Research 2010; **40**: 432–437 doi: 10.1111/j.1872-034X.2009.00612.x

Short Communication

Expression of the RNA-binding protein Musashi1 in adult liver stem-like cells

Etsuko Hattori,[1,*] Hong-Jin Shu,[1,*] Takafumi Saito,[1] Kazuo Okumoto,[1] Hiroaki Haga,[1] Junji Yokozawa,[1] Junitsu Ito,[1] Hisayoshi Watanabe,[1] Koji Saito,[1] Hitoshi Togashi[2] and Sumio Kawata[1]

[1]*Department of Gastroenterology, Yamagata University School of Medicine, and* [2]*Health Administrative Center, Yamagata University, Yamagata, Japan*

Aim: Musashi1 is an RNA-binding protein that regulates the Notch signaling pathway in stem cells. Our previous study revealed that Musashi1 is expressed in early hepatocytes during liver development in the mouse. However, whether this unique protein is expressed with Notch signaling markers in adult liver stem-like cells remains unknown.

Methods: Established hepatic stem-like cells (HSLC), which were derived from adult Sprague–Dawley rats, were used for experiments *in vitro*. HSLC were differentiated into mature cells in terms of producing albumin when co-cultured with epidermal growth factor (EGF). The mRNA expression of *Musashi1*, *Notch* family (*Notch1* and *Notch2*), *Jagged1* and *Hes1* was examined in HSLC before and after cell differentiation using polymerase chain reaction-based techniques. Protein expression of Musashi1 was examined in the HSLC and normal mature hepatocytes by immunofluorescence staining.

Results: The mRNA expression of *Musashi1*, *Notch1*, *Jagged1* and *Hes1* was detected in the original HSLC before culturing with EGF but not in primary cultured mature hepatocytes. The mRNA expression of *Musashi1* and *Hes1* was found to be downregulated in differentiated HSLC that produce albumin. Protein expression of Musashi1 was detectable in the original HSLC but not in both differentiated HSLC and mature hepatocytes.

Conclusion: These findings demonstrate that the RNA-binding protein Musashi1 is expressed with Notch signaling markers in adult liver stem-like cells.

Key words: hepatic stem cell, Musashi1, Notch, liver, RNA-binding protein

INTRODUCTION

IT HAS BEEN demonstrated that liver cell regeneration originates from epithelial cells through two mechanisms. First, mature hepatocytes can proliferate independently by division after the loss of liver cells, as is often observed after a partial hepatectomy.[1] An alternative mechanism, in which liver stem/progenitor cells that subsequently differentiate into hepatocytes, cholangiocytes or other liver components are produced, is involved in reconstruction of the liver after severe liver damage.[2] The signal transduction in liver stem cell differentiation has not been fully investigated.

Correspondence: Dr Takafumi Saito, Department of Gastroenterology, Yamagata University School of Medicine, 2-2-2 Iida-nishi, Yamagata 990-9585, Japan. Email: tasaitoh@med.id.yamagata-u.ac.jp
*The first two authors contributed equally to this work
Received 25 February 2009; revision 2 September 2009; accepted 11 September 2009.

Musashi1, a neural RNA-binding protein was first isolated as a mammalian homolog of the *Drosophila* protein, which is required for the asymmetric division of sensory neural precursor cells.[3] It is also known that Musashi1 is a positive regulator of the Notch signaling pathway,[4,5] which is essential for the determination of cell fate,[6] thereby maintaining the self-renewing ability of stem cells. Thus, Musashi1 is closely involved in the regulation of asymmetric cell division of stem-like cells, which generates differentiated cells.

In our previous study, we have shown that Musashi1 is expressed in early hepatocytes during liver development in the mouse.[7] Whether this unique RNA-binding protein has any association with the process of liver stem cell differentiation in adults is of considerable interest. In this study, we investigated the expression of Musashi1 in adult liver stem-like cells that regulates the Notch signaling. Our results suggest a possible association of Musashi1 in liver stem-like cell differentiation.

METHODS

Liver stem cell line and culture

AN ESTABLISHED HEPATIC epithelial stem-like cell (HSLC) line derived from the healthy liver of adult male Sprague–Dawley rats[8] was used for experiments *in vitro*. This cell line has an immature liver cell phenotype with positive expression only for α-fetoprotein and negative for both albumin and cytokeratin (CK)19, and exhibits the potential to differentiate into cells of the hepatocytic lineage and serve as stem-like cells for differentiated hepatocytes.[8] The cells were maintained in Dulbecco's modified Eagle's medium supplemented with 10% fetal bovine serum at 37°C. Spheroidal aggregates of hepatocytes are known to exhibit higher functions than hepatocytes produced by monolayer culture.[9,10] In order to demonstrate the differentiation of HSLC into cells of the hepatocytic lineage *in vitro*, the cells were co-cultured for 24 h with epidermal growth factor (EGF) at a concentration of 10 ng/mL. These cells formed spheroids in culture. The expression of albumin was examined as a marker of cell differentiation in culture cells. The mRNA expression profile for both CK19 and tyrosine aminotransferase (TAT) was also examined in HSLC before and after culturing with EGF. Primary cultured, normal adult hepatocytes were used as control cells.[11]

Western blot analysis of albumin expression in HSLC

Expression of albumin was analyzed in HSLC cultured with or without EGF. The proteins were prepared by treating the cells with cell lysis buffer, followed by centrifugation. A 15-μg sample of proteins was subjected to a 10% sodium dodecylsulfate polyacrylamide ready gel (Bio-Rad Laboratories, Richmond, CA, USA). Resolved proteins were transferred electrophoretically to an Immunobilon-P membrane (Millipore, Bedford, MA, USA) at 4°C and processed for immunodetection. After blocking with 5% nonfat milk for 1 h at room temperature, the membrane was incubated with rabbit antirat albumin antibody (1:200 dilution; Cappel, Aurora, OH, USA) at 37°C for 2.5 h. The membrane was then incubated with alkaline phosphatase-labeled goat antirabbit immunoglobulin (Ig)G antibody (1:1000 dilution; KPL, Gaithersburg, MD, USA) for 1.5 h at room temperature. Detection of the immunoreaction was performed with the BCIP/NBT phosphate substrate system (KPL), according to the manufacturer's protocol.

Reverse transcription polymerase chain reaction (RT–PCR)

The mRNA expression of *CK19*, *TAT*, *Notch* family (*Notch1* and *Notch2*) and its ligand *Jagged1*, and *Hes1* in both HSLC cultured with or without EGF and in primary cultured mature hepatocytes were examined by RT–PCR according to the procedure we previously described.[7] The PCR consisted of 35 cycles at a denaturation temperature of 94°C for 30 s, an annealing temperature of 58°C for 2 min and an extension temperature of 72°C for 1 min using a Perkin-Elmer 9600 thermal cycler platform (Perkin-Elmer, Norwalk, CT, USA). The primers for PCR to detect mRNA expression were: *Musashi1*, 5′-GGC TTCGTCACTTTCATGGACCAGGCG-3′ and 5′-GGGACC TGGTAGGTGTAAC-3′ (PCR product; 542 bp); *Hes1*, 5′-CCACTGCTACCCGTAAAGTC-3′ and 5′-GGCCTGAG GCTCTCAGTTCC-3′ (228 bp); *Notch1*, 5′-GACTATGCC TGCAGCTGTGCC-3′ and 5′-GGCTGCAGGGCACGTA GG-3′ (421 bp); *Notch2*, 5′-ATGTGTGTTACCTACCA CA-3′ and 5′-CCACAGTGGTACAGGTACTT-3′ (371 bp); *Jagged1*, 5′-CATCATAGCCTGTGAGCCTTC-3′ and 5′-ATATCATCCTCTTCCACTTCC-3′ (492 bp); CK19, 5′-TT GCGCGACAAGATTCTTGG-3′ and 5′-CATCTCACTCAG GATCTTGG-3′ (361 bp); and TAT, 5′-TGAACAGCAC TACCACTGTG-3′ and 5′-AGGCATCCTCCGTCTTCT GC-3′ (380 bp). The PCR reaction for β-actin was performed as an internal control (191 bp).[7]

Quantitation of Musashi1 mRNA levels in HSLC before and after differentiation

The total cellular RNA extracted from Hep3B cells positive for *Musashi1* mRNA expression[7] was used as a standard. The methods for RNA isolation and cDNA amplification were performed as previously.[7] To quantitate *Musashi1* mRNA levels in HSLC before and after differentiation, real-time PCR was performed using a LightCycler quick system 350S (Roche Diagnostics, Tokyo, Japan) according to the manufacturer's instructions. The primers for detection of *Musashi1* mRNA in the real-time PCR were 5′-GGCTTCGTCACTTTCATGGA CCAGGCG-3′ and 5′-GGGACCTGGTAGGTGTAAC-3′. Quantitation test was performed in quadruplicate and the results were expressed as mean ± standard error (SE). Differences at $P < 0.05$ by Mann–Whitney *U*-test were considered significant.

Immunofluorescence staining for Musashi1 in HSLC

Expression of Musashi1 was analyzed by indirect immunofluorescence staining in HSLC cultured with or

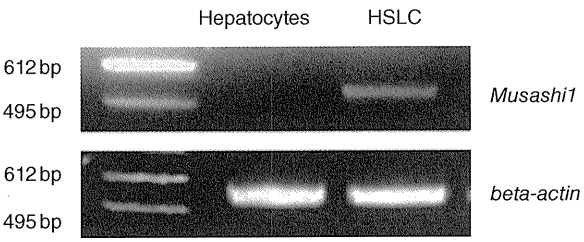

Figure 1 Reverse transcription polymerase chain reaction (RT–PCR) analysis of *Musashi1* mRNA expression in hepatic stem-like cells (HSLC) and primary cultured mature hepatocytes. The mRNA expression of *Musashi1* was detected in HSLC but not in hepatocytes. The predicted size of the PCR-amplified *Musashi1* product was 542 bp.

without EGF. A polyclonal rabbit anti-Musashi peptide antibody (Chemicon International, Temecula, CA, USA) that recognizes human and rodent Musashi1 was used as a primary antibody. Fluorescein isothiocyanate-labeled $F(ab')_2$ fragments of goat antirabbit IgG (Dako-Cytomation, Kyoto, Japan) were used as a secondary antibody. The cells were examined with the aid of a fluorescence microscope.

RESULTS

Expression of Musashi1 mRNA and Musashi1 protein in HSLC

THE MRNA EXPRESSION of *Musashi1* was detected in HSLC but not in primary cultured mature hepatocytes by RT–PCR (Fig. 1). The RT–PCR product of the *Musashi1* mRNA amplified using specific primers predicted a band of 542 bp. Protein expression of Musashi1 was detected in HSLC by immunofluorescence staining (Fig. 2), but it was not detected in primary cultured hepatocytes.

Downregulated expression of Musashi1 mRNA and Musashi1 protein in differentiated HSLC producing albumin

Hepatic stem-like cells were cultured with 10 ng/mL EGF for 24 h and harvested when they formed spheroids. Albumin expression in these cells was examined as a marker of cell differentiation from an immature to a mature state. Albumin expression was not detected in HSLC before culturing with EGF, but was detectable by western blot analysis after culturing with EGF. Quantitative analysis revealed that the level of *Musashi1* mRNA in the differentiated HSLC was significantly lower than that of original HSLC ($1.06 \pm 1.34 \times 10^{10}$ copies/mL vs $4.33 \pm 2.68 \times 10^{13}$ copies/mL, mean ± SE, $P < 0.05$) (Fig. 3). Expression of Musashi1 protein was not detected in differentiated HSLC producing albumin by immunofluorescence staining.

Changes in mRNA expression of the Notch signaling markers in HSLC differentiation

Because the expression of *Musashi1* mRNA was found to be downregulated in the cell differentiation process, the expression of the *Notch* family mRNA was investigated in HSLC before and after culturing with EGF by RT–PCR analysis. *Notch1* mRNA expression was detected in HSLC before and after culturing with EGF, but its expression was not detected in primary cultured mature hepatocytes. *Notch2* mRNA expression was found in HSLC before and after culturing with EGF as well as in primary cultured mature hepatocytes. The notch ligand *Jagged1* mRNA expression was detected in HSLC before and after culturing with EGF, but its expression was not detected in primary cultured mature hepatocytes. *Hes1* mRNA expression was detected in the original HSLC, but not in those producing albumin after culturing with EGF, and nor was it detected in primary cultured mature hepatocytes. The biliary cell marker, CK19 mRNA expression was not detected in any cells examined. The hepatocyte marker, TAT mRNA expression was not detected in the original HSLC, but its expression was detectable in those

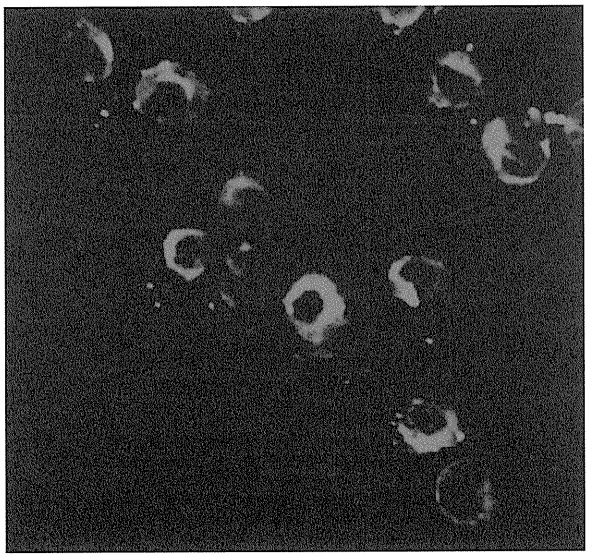

Figure 2 Immunofluorescence staining for Musashi1 protein in the cytoplasm of hepatic stem-like cells (original magnification ×400).

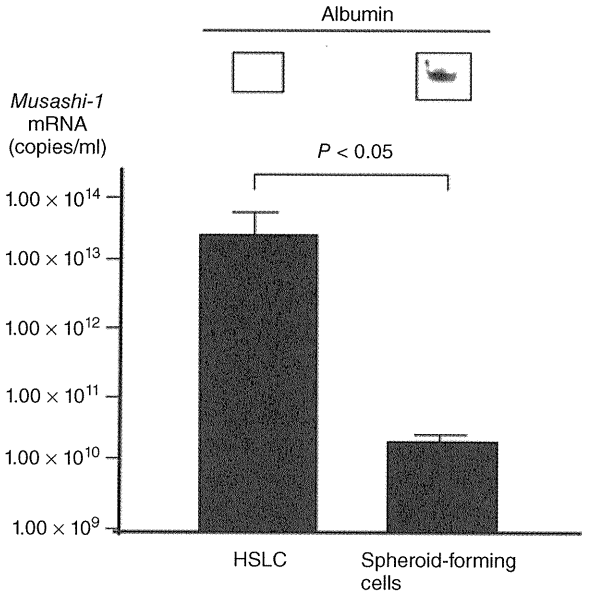

Figure 3 Western blot analysis of albumin expression in hepatic stem-like cells (HSLC). Albumin expression was not detected in the original HSLC, but was detected in spheroid-forming cells after culturing with epidermal growth factor (EGF). Real-time polymerase chain reaction analysis of *Musashi1* mRNA expression in HSLC before and after culturing with EGF. The level of *Musashi1* mRNA in the spheroid-forming differentiated cells was significantly lower than that of original HSLC. Quantitation test was performed in quadruplicate.

producing albumin after culturing with EGF as well as in primary cultured mature hepatocytes (Fig. 4).

DISCUSSION

ALTHOUGH A CLOSE association has been shown to exist between Musashi1 and Notch signaling in neural stem cell differentiation,[4] the involvement of such a mechanism in the differentiation of stem cells in digestive organs has not been fully elucidated. Recently, it was shown that Musashi1 is expressed in putative intestinal stem cells [12] and can be used as a marker of stem cells and early-lineage progenitor cells in murine intestinal tissue.

In this study, we have demonstrated that Musashi1 is expressed in putative rat liver stem-like cells at the mRNA and protein level. Interestingly, the mRNA expression of *Hes1* was downregulated along with *Musashi1* mRNA expression in the differentiated cells that produced albumin. Notch proteins were initially identified in *Drosophila* and *Caenorhabditis elegans*, but have subsequently been identified in vertebrate species.[13] It has been reported that there is an association between expression of the *Notch* family, and bile duct formation,[14] liver cell regeneration after partial hepatectomy[15] and neovascularization in the human diseased liver,[16] although no such association has been demon-

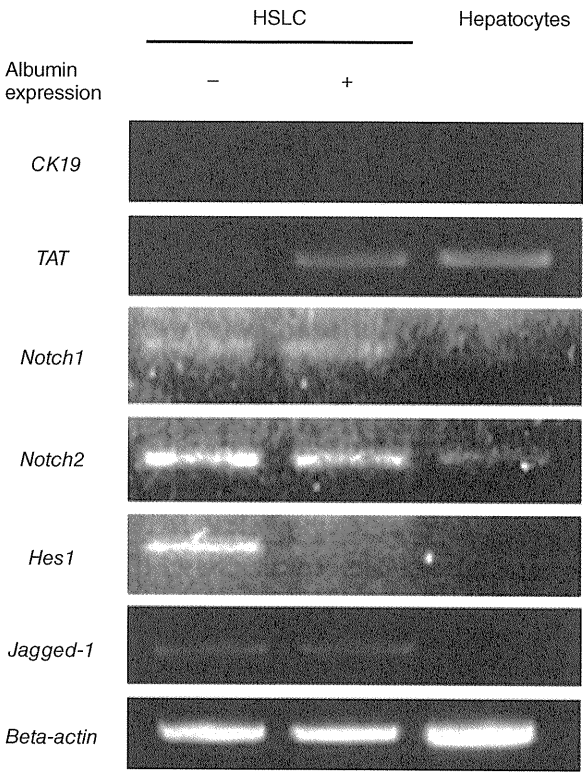

Figure 4 The mRNA expression for cytokeratin (CK)19, tyrosine aminotransferase (TAT) and *Notch* family in hepatic stem-like cells (HSLC), as revealed by reverse transcription polymerase chain reaction (RT–PCR) analysis. CK19 mRNA expression was not detected in all cells. TAT mRNA expression was not detected in the original HSLC, but it was detectable in differentiated cells producing albumin as well as in mature hepatocytes. The mRNA expression for *Notch1* and *Jagged1* was detected in HSLC, but it was not detected in mature hepatocytes. *Notch2* mRNA expression was detected in all cells. The mRNA expression of *Hes1* was detected in HSLC, but was undetectable in differentiated cells producing albumin as well as in mature hepatocytes. The predicted size of the PCR-amplified product was 361 bp for CK19, 380 bp for TAT, 421 bp for *Notch1*, 371 bp for *Notch2*, 492 bp for *Jagged-1* and 228 bp for *Hes1*.

strated in liver stem cells. Both Notch-1 and its ligand Jagged-1 have been detected in the hepatic progenitor cells, referred to as oval cells, in the liver of the 2-acetylaminofluorene 70% hepatectomy models.[17] In this study, *Notch1* and *Jagged1* mRNA expressions were detectable in HSLC , but not in mature rat hepatocytes. The absence of Notch1 expression in mature hepatocytes has also been demonstrated in humans.[17] *Hes1* mRNA expression is activated by a nuclear translocation of the Notch intracellular domain.[11] In the present study, we could show that *Hes1* mRNA expression was also detectable in HSLC at a location downstream of this signaling. The mRNA expression of *Notch1–Hes1* signaling was upregulated in Musashi1-positive HSLC and was undetectable in the differentiated cells producing albumin. To confirm the association of Musashi1 with an activation of the Notch signaling, it would be important to see if changes in Musashi1 expression level by the gene knockdown influence of liver stem-like cell differentiation. In addition, expression of Musashi1 in the liver tissue remains unknown. Further studies are needed to elucidate these issues.

The roles of Musashi1 in the development of liver morphology and function remain unknown. A report on the *Musashi1* gene disruption model revealed that homozygous newborn mice are not prone to immediate death, but frequently develop obstructive hydrocephalus with aberrant proliferation of ependymal cells.[5] As Musashi2, another member of the RNA-binding protein family,[18] is co-expressed in this model, gene compensation of *Musashi2* in the *Musashi1* disruption model might contribute to organ development, and hence improve the chances of survival. Analyses of alteration of liver-specific mRNA expression as well as liver morphology in such a model would provide information that could extend our understanding of the role of Musashi1 in the development of liver morphology and function.

In conclusion, the results of this study suggest that Musashi1 is expressed with Notch signaling markers in liver stem-like cells as well as in neural stem cells in adults. The role of Musashi1 in liver regeneration warrants further investigation.

ACKNOWLEDGEMENTS

THE AUTHORS THANK Dr Toshihiro Sugiyama for the gift of HSLC and Dr Hideyuki Okano for critical reading of the manuscript. This paper was supported by a Grant-in-Aid from the Global COE program of the Japan Society for the Promotion of Science, and in part by a grant from the Ministry of Health, Labor and Welfare of Japan.

REFERENCES

1 Bucher NL. Experimental aspects of hepatic regeneration. *N Engl J Med* 1967; **277**: 686–96.
2 Thorgeirsson SS. Hepatic stem cells in liver regeneration. *FASEB J* 1996; **10**: 1249–56.
3 Nakamura M, Okano H, Blendy JA, Montell C. Musashi, a neural RNA-binding protein required for Drosophila adult external sensory organ development. *Neuron* 1994; **13**: 67–8.
4 Okano H, Imai T, Okabe M. Musashi: a translational regulator of cell fate. *J Cell Sci* 2002; **115**: 1355–9.
5 Imai T, Tokunaga A, Yoshida T *et al.* The neural RNA-binding protein Musashi1 translationally regulates mammalian numb gene expression by interacting with its mRNA. *Mol Cell Biol* 2001; **21**: 3888–900.
6 Artavanis-Tsakonas S, Rand MD, Lake RJ. Notch signaling: cell fate control and signal integration in development. *Science* 1999; **284**: 770–6.
7 Shu HJ, Saito T, Watanabe H *et al.* Expression of the Musashi1 gene encoding the RNA-binding protein in human hepatoma cell lines. *Biochem Biophys Res Commun* 2002; **293**: 150–4.
8 Nagai H, Terada K, Watanabe G, *et al.* Differentiation of liver epithelial (stem-like) cells into hepatocytes induced by coculture with hepatic stellate cells. *Biochem Biophys Res Commun* 2002; **293**: 1420–5.
9 Matsushita T, Ijima H, Koide N, Funatsu K. High albumin production by multicellular spheroid of adult rat hepatocytes formed in the pores of polyurethane foam. *Appl Microbiol Biotechnol* 1991; **36**: 324–6.
10 Tobe S, Takei Y, Kugumiya T, Kobayashi A, Kobayashi K, Akaike T. Formation mechanism and differential functionality of multiplayer hepatocyte-aggregation on artificial biomatrix. *Jpn J Artif Organs* 1992; **20**: 150–5.
11 Okumoto K, Saito T, Hattori E *et al.* Differentiation of bone marrow cells into cells that express liver-specific genes *in vitro*: implication of the Notch signals in differentiation. *Biochem Biophys Res Commun* 2003; **304**: 691–5.
12 Potten CS, Booth C, Tudor GL *et al.* Identification of a putative intestinal stem cell and early lineage marker; musashi-1. *Differentiation* 2003; **71**: 28–41.
13 Weinmaster G. The ins and outs of Notch signaling. *Mol Cell Neurosci* 1997; **9**: 91–102.
14 Kodama Y, Hijikata M, Kageyama R, Shimotohno K, Chiba T. The role of notch signaling in the development of intrahepatic bile ducts. *Gastroenterology* 2004; **127**: 1775–86.
15 Kohler C, Bell AW, Bowen WC, Monga SP, Fleig W, Michalopoulos GK. Expression of Notch-1 and its ligands Jagged-1 in rat liver during liver regeneration. *Hepatology* 2004; **39**: 1056–65.

16 Nijjar SS, Crosby HA, Wallace L, Hubscher SG, Strain AJ. Notch receptor expression in adult human liver: a possible role in bile duct formation and hepatic neovascularization. *Hepatology* 2001; **34**: 1184–92.
17 Jensen CH, Jauho EI, Santoni-Rugiu E *et al.* Transit-amplifying ductular (oval) cells and their hepatocytic progeny are characterized by a novel and distinctive expression of delta-like protein/preadipocyte factor 1/fetal antigen 1. *Am J Pathol* 2004; **164**: 1347–1359.
18 Sakakibara S, Nakamura Y, Satoh H, Okano H. RNA-binding protein Musashi2: developmentally regulated expression in neural precursor cells and subpopulations of neurons in mammalian CNS. *J Neurosci* 2001; **21**: 8091–107.

Journal of Medical Virology 82:1364–1370 (2010)

Secondary Structure of the Amino-Terminal Region of HCV NS3 and Virological Response to Pegylated Interferon Plus Ribavirin Therapy for Chronic Hepatitis C

Mai Sanjo,[1] Takafumi Saito,[1]* Rika Ishii,[1] Yuko Nishise,[1] Hiroaki Haga,[1] Kazuo Okumoto,[1] Junitsu Ito,[1] Hisayoshi Watanabe,[1] Koji Saito,[1] Hitoshi Togashi,[2] Kazuto Fukuda,[3] Yasuharu Imai,[3] Ahmed El-Shamy,[4] Lin Deng,[4] Ikuo Shoji,[4] Hak Hotta,[4] and Sumio Kawata[1]

[1]*Department of Gastroenterology, Yamagata University School of Medicine, Yamagata, Japan*
[2]*Health Administrative Center, Yamagata University, Yamagata, Japan*
[3]*Division of Gastroenterology, Ikeda Municipal Hospital, Osaka, Japan*
[4]*Division of Microbiology, Kobe University Graduate School of Medicine, Kobe, Japan*

The aim of the study was to identify a predictive marker for the virological response in hepatitis C virus 1b (HCV-1b)-infected patients treated with pegylated interferon plus ribavirin therapy. A total of 139 patients with chronic hepatitis C who received therapy for 48 weeks were enrolled. The secondary structure of the 120 residues of the amino-terminal HCV-1b non-structural region 3 (NS3) deduced from the amino acid sequence was classified into two major groups: A and B. The association between HCV NS3 protein polymorphism and virological response was analyzed in patients infected with group A (n = 28) and B (n = 40) isolates who had good adherence to both pegylated interferon and ribavirin administration (>95% of the scheduled dosage) for 48 weeks. A sustained virological response (SVR) representing successful HCV eradication occurred in 33 (49%) in the 68 patients. Of the 28 patients infected with the group A isolate, 18 (64%) were SVR, whereas of the 40 patients infected with the group B isolate only 15 (38%) were SVR. The proportion of virological responses differed significantly between the two groups ($P < 0.05$). These results suggest that polymorphism in the secondary structure of the HCV-1b NS3 amino-terminal region influences the virological response to pegylated interferon plus ribavirin therapy, and that virus grouping based on this polymorphism can contribute to prediction of the outcome of this therapy. ***J. Med. Virol. 82:1364–1370, 2010.*** © 2010 Wiley-Liss, Inc.

KEY WORDS: hepatitis C; interferon; ribavirin; interaction; polymorphism

INTRODUCTION

Hepatitis C virus (HCV) is the major pathogen that causes chronic liver diseases with a risk of progression to cirrhosis and hepatocellular carcinoma. Currently, the standard treatment for chronic hepatitis C is antiviral therapy using pegylated interferon (Peg-IFN) plus ribavirin (RBV), and this approach is most effective for eradication of HCV viremia. However, even with the widely used treatment regimen of 48 weeks, the rate of sustained virological response (SVR), which indicates eradication of viremia, is still approximately 50% for patients infected with the therapy-resistant HCV genotype 1b (HCV-1b) with a high viral load [Manns et al., 2001; Bruno et al., 2004; Hadziyannis et al., 2004]. It would be useful to predict the virological response to this therapy and to identify patients who would obtain beneficial therapeutic effects before treatment, in order to avoid any serious side effect and to eliminate those who would not be helped by the treatment. In the future it will be important to establish a protocol of tailor-made medicine for chronic hepatitis C.

Grant sponsor: Grant-in-Aid for Scientific Research; Grant number: 21590824; Grant sponsor: Global Center of Excellence program of the Japan Society for the Promotion of Science (Yamagata University School of Medicine and Kobe University Graduate School of Medicine); Grant sponsor: Ministry of Health, Labor and Welfare of Japan.

*Correspondence to: Takafumi Saito, M. D., Department of Gastroenterology, Yamagata University School of Medicine, 2-2-2 Iida-nishi, Yamagata 990-9585, Japan.
E-mail: tasaitoh@med.id.yamagata-u.ac.jp

Accepted 6 March 2010

DOI 10.1002/jmv.21818

Published online in Wiley InterScience (www.interscience.wiley.com)

Both the HCV genotype and pre-treatment viral load are major viral factors that influence the response to IFN-based antiviral therapy, but IFN resistance is also partly due to variation of the amino acid sequence encoded by HCV itself. Enomoto et al. [1996] proposed that variation of 40 amino acids within the NS5A region (aa 2,209–2,248), which is referred to as the IFN sensitivity-determining region (ISDR), is well correlated with IFN responsiveness. ISDR and its adjacent sequence bind and inhibit the enzymatic activity of a double-stranded RNA-activated protein kinase (PKR), which can have an antiviral effect, and therefore the combined region is referred to as the PKR-binding domain (PKR-BD) [Gale et al., 1997, 1998]. A correlation between sequence variation in the PKR-BD and IFN responsiveness has been reported [Nousbaum et al., 2000], and some reports show a correlation between IFN responsiveness and the sequence diversity of variable region 3 (V3) (aa 2,356–2,379) or surrounding regions near the carboxy terminus of NS5A [Murphy et al., 2002; Sarrazin et al., 2002; Puig-Basagoiti et al., 2005]. A high degree of amino acid substitution in the V3 and pre-V3 regions (aa 2,334–2,355) of NS5A, which is referred to as the IFN/RBV resistance-determining region (IRRDR) (aa 2,334–2,379), has been associated with SVR in Peg-IFN/RBV combination therapy for patients infected with HCV-1b [El-Shamy et al., 2007, 2008]. In addition to these findings in non-structural proteins of the virus, amino acid substitution in a structural region of HCV has been reported to be a predictive viral marker for the virological response to PegIFN/RBV therapy. Amino acid polymorphisms in the HCV core region (Arg70 vs. Gln70 and Leu91 vs. Met91) correlate with virological outcome and on-treatment viral kinetics in Peg-IFN/RBV therapy [Akuta et al., 2006, 2007], and a double wild-type HCV core (Arg70 and Leu91) may be a significant predictor of SVR in Peg-IFN/RBV therapy [Akuta et al., 2007].

Interactions between viral and host proteins in infected cells may influence therapeutic effects and the natural history of infection, since the HCV NS3 region has a significant effect on immunity. The amino-terminal part of this region encodes a serine protease, for which the minimum activity has been mapped to a region between aa 1,059 and 1,204 [Yamada et al., 1998]. The serine protease inactivates Cardif, a caspase recruitment domain (CARD)-containing adaptor protein that interacts with the RNA helicase retinoic acid inducible gene 1 (RIG-1)-dependent antiviral pathway in infected cells [Foy et al., 2003; Meylan et al., 2005; Evans and Seeger, 2006]. This action inhibits phosphorylation and subsequent heterodimerization of interferon regulatory factor-3 (IRF-3), which is essential for activation of IFN signaling through translocation of IRF-3 heterodimers into the nucleus, and eventually blocks IFN-beta production. In addition, inactivation of IRF-3 is postulated to influence the therapeutic effect of IFN-based antiviral therapy, because the IRF-3 heterodimer translocates into the nucleus to bind to the IFN-stimulated response element that produces many antiviral proteins, including 2′,5′-oligoadenylate synthetase and PKR [Nakaya et al., 2001; Grandvaux et al., 2002]. Collectively, these findings suggest that polymorphisms in HCV NS3 structure deduced from sequence variation may influence IFN-related signaling and the antiviral effect of IFN-based anti-HCV therapy.

We have focused on polymorphisms in the secondary structure of the viral polyprotein that interacts with host proteins involved in immunity, with the aim of identification of predictive viral markers for the response to Peg-IFN/RBV therapy. In this study, we examined the potential correlation between polymorphisms in the secondary structure of the HCV NS3 amino-terminal region and virological responses to Peg-IFN/RBV therapy in patients infected with HCV-1b with a high viral load.

PATIENTS AND METHODS

Patients and Treatment Regimen With Peg-IFN Plus Ribavirin

A total of 139 consecutive patients diagnosed with chronic hepatitis C were enrolled in the study from December 2004 to March 2007. These patients included 81 men and 58 women, and were aged from 31 to 75 years old (mean ± SD, 56.8 ± 8.7 years old). All patients were infected with HCV-1b with a high viral load of over 100 KIU/ml, and all received Peg-IFN/RBV therapy. Patients with alcoholic liver injury, autoimmune liver disease, and those who had symptoms of decompensated cirrhosis including ascites were excluded. Briefly, all patients were treated with a combination of Peg-IFN-alpha 2b (Pegintron®; Schering-Plough, Kenilworth, NJ) and RBV (Rebetol®; Schering-Plough) for 48 weeks. Peg-IFN was administered subcutaneously once a week and RBV was given orally twice a day for the total dose. The dosages were determined on the basis of body weight according to the Japanese standard prescription information supplied by the Japanese Ministry of Health, Labour and Welfare, and there was a limit for calculating the optimized dose: patients with body weights of 35–45, 46–60, 61–75, and 76–90 kg were given Peg-IFN at doses of 60, 80, 100, and 120 μg, respectively, and those with body weights of <60, 60–80, and >80 kg were given RBV at doses of 600, 800, and 1,000 mg, respectively. The dose of Peg-IFN or RBV was reduced according to the Japanese standard criteria based on the white blood cell count, neutrophil count, hemoglobin concentration and platelet count [Hiramatsu et al., 2008].

Virological Tests and Response to Peg-IFN Plus Ribavirin

Virological responses were evaluated at 12 weeks after the start of treatment with an early depletion of viremia referred to as an early virological response (EVR), at the end of treatment with depletion of viremia referred to as an end of treatment virological response (ETR), and at 24 weeks after completion of treatment,

with a clinical outcome of a sustained virological response (SVR) representing successful HCV eradication. All patients were negative for hepatitis B surface antigen. Quantification of serum HCV RNA was performed using an RT-PCR-based commercial kit (Amplicor HCV monitor test, ver. 2.0, Roche Diagnostics, Tokyo, Japan). This Amplicor HCV RNA assay has a lower limit of detection of 50 IU/ml. SVR was determined by monitering negativity for HCV RNA monthly for 6 months. The real-time PCR assay kit (COBAS TaqMan HCV Auto, Roche Diagnostics) for more precise quantitation of HCV viremia has recently become available and pre-treatment viral titers were re-evaluated using preserved serum samples. This real-time PCR assay has a lower limit of detection of 15 IU/ml. The study protocol was approved by the Ethics Committee of Yamagata University Hospital. Informed consent was obtained from all patients.

PCR Amplification of the Amino-Terminal Region of NS3

RNA was extracted from 50 μl of serum using an RNeasy Mini kit (Qiagen, Tokyo, Japan). To amplify the region of the HCV genome encoding the amino-terminal region of NS3 (1,027–1,206), a one-step PCR was performed in a tube using the Superscript One-Step RT-PCR kit with Platinum Taq (Gibco-BRL, Tokyo, Japan) and an outer set of primers: NS3-F1 (sense primer; 5′-ACA CCG CGG CGT GTG GGG ACA T-3′; nucleotides 3,295–3,316) and NS3-AS2 (antisense primer; 5′-GCT CTT GCC GCT GCC AGT GGG A-3′; nucleotides 4,040–4,019), as reported previously [Ogata et al., 2002a, 2003]. PCR was initially performed at 45°C for 30 min at RT and then at 94°C for 2 min, followed by the first-round PCR for forty 3-min cycles at 94°, 55°, and 72°C for 1 min each. The second-round PCR was performed with *Pfu* DNA polymerase (Promega, Tokyo, Japan) and an inner set of primers: NS3-F3 (sense primer; 5′-CAG GGG TGG CGG CTC CTT-3′; nucleotides 3,390–3,407) and NS3-AS1 (antisense primer; 5′-GCC ACT TGG AAT GTT TGC GGT A-3′; nucleotides 4,006–3,985). The second-round PCR was performed for 35 cycles, with each cycle consisting of 1 min at 94°C, 1.5 min at 55°C, and 3 min at 72°C. This method allowed amplification of the corresponding portion of the HCV genome from HCV-1b RNA-positive samples. The amplified fragments were purified with a QIAquick PCR purification kit (Qiagen) and directly sequenced (without being subcloned) in both directions using a dRhodamine Terminator Cycle Sequencing Ready Reaction kit and an ABI 377 sequencer (Applied Biosystems, Tokyo, Japan).

Classification of the Secondary Structure of the HCV-1b NS3 Amino-Terminal Region

The secondary structure of the amino-terminal region of HCV NS3 was predicted by computer-assisted Robson analysis [Garnier et al., 1978] with Genetyx-Mac software (ver.10.1; Software Development Co., Tokyo, Japan). Previously, the full-length secondary structure of the HCV-1b NS3 region was analyzed, and this showed that the secondary structure deduced from the carboxy-terminal 60 residues was well conserved in terms of linear structure, without any turn structure [Ogata et al., 2002a]. We have shown that the secondary structure of the 120 residues in the amino-terminal region of HCV-1b NS3 can be classified into two major groups: A and B (Fig. 1) [Ogata et al., 2002a, 2003]. Briefly, the criteria for this classification are as follows: in group A isolates, the carboxy-terminal 20 residues (aa 1,125–1,146) are oriented leftward relative to a domain composed of the remaining amino-terminal region; whereas in group B isolates, the same 20 residues are oriented rightward relative to the rest of the amino-terminal domain.

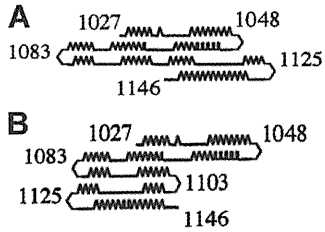

Fig. 1. Secondary structure of the 120 amino-terminal residues of HCV-1b nonstructural 3 (NS3) region classified into two major groups: A and B. The looped, zigzag, straight, and bent lines represent α-helix, β-sheet, coil, and turn structures, respectively. The numbers indicate amino acid positions. **A**: Group A, (**B**) Group B.

Analysis of Amino Acid Substitutions in the Core Region

To amplify a region of the HCV genome encoding the core region including positions 70 and 91, reverse transcription and the first-round PCR were performed in a tube by the Superscript One-Step RT-PCR kit with Platinum *Taq* (Gibco-BRL) and an outer set of primers, followed by second-round PCR with an inner set of primers in accordance with procedures reported previously [Ogata et al., 2002b]. The sequences of the amplified fragments were determined by direct sequencing.

Statistical Analysis

Data were analyzed by a χ^2 test for independence with a two-by-two contingency table and a Student t-test. A P-value <0.05 was considered significant.

RESULTS

Virological Response *and Adherence* to the Peg-IFN Plus Ribavirin Regimen

Rates of virological responses in patients treated with PegIFN/RBV combination therapy for 48 weeks are shown in Figure 2. Of the 139 patients enrolled in the study, SVR, non-SVR and cessation of therapy occurred in 58 (42%), 62 (45%), and 19 (14%), respectively. Serious

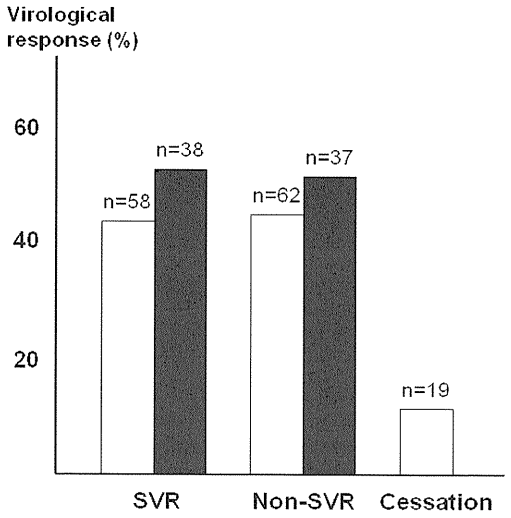

Fig. 2. Virological response in patients treated with peginterferon plus ribavirin for 48 weeks. The results are shown for all 139 subjects (open bars) and for 75 cases with good adherence of >80% of the scheduled dosages (closed bars). SVR, sustained virological response.

adverse events that necessitated discontinuation of this therapy were depression in one patient, thyroid function disorder in 2, general itching in 2, infection in 2, anorexia in 2, occurrence of hepatocellular carcinoma in 2, and a decreased neutrophil count in 2. Six patients also terminated this therapy at their own request. Of the 139 patients, 75 (54%) received >80% of the scheduled dosage of Peg-IFN and RBV designated before treatment, and of these 75 cases SVR and non-SVR occurred in 38 (51%) and 37 (49%), respectively.

Prevalence of Types of Secondary Structure of the Amino-Terminal Region of HCV NS3

The prevalence of the types of secondary structure of HCV NS3 in the 139 subjects is shown in Table I. Among these subjects, 43 (31%), 70 (50%), and 26 (19%) were classified into groups A, B, and others, including 3 of mixed type (A plus B) and 23 of non-A, non-B type. Of the 75 cases with good adherence to administration of >80% of the scheduled dosage, 28 (37%), 40 (53%) and 7 (9%) were classified into groups A, B, and others. The amino acid data of group A and B in the cases with good adherence to administration are available in the DDBJ/EMBL/GenBank databases with the accession numbers AB548070–AB548137. Our analysis revealed no specific correlations between amino acid sequences and the secondary structure deduced by the Robson method, as we have reported previously [Ogata et al., 2003].

TABLE I. Prevalence of the HCV NS3 Secondary Structure Type

	Group A (%)	Group B (%)	Others (%)
Enrolled cases (n = 139)	43 (31)	70 (50)	26 (19)
Adherent cases (n = 75)	28 (37)	40 (53)	7 (9)

Characteristics of Adherent Patients Based on Different HCV NS3 Structure Types

The virological responses to Peg-IFN/RBV combination therapy for patients infected with group A and B isolates were assessed in the 68 subjects with good adherence to the scheduled dosage of Peg-IFN and RBV. The characteristics of patients infected with group A and B isolates are shown in Table II. Age, gender, pre-treatment level of serum HCV RNA and ALT, and frequency of fibrosis stage did not differ significantly between the two groups. Peg-IFN/RBV combination therapy was completed in all the patients, and the total administered dosages of Peg-IFN and RBV was >95% of the scheduled dosage in both groups.

Relationship Between Virological Responses and Polymorphisms in the HCV NS3 Amino-Terminal Region

In the 68 patients who received >95% of the scheduled doses of Peg-IFN and RBV for 48 weeks, SVR and non-SVR occurred in 33 (49%) and 35 (51%), respectively. The EVR, ETR, and SVR rates in patients infected with group A and B isolates are shown in Table III. There was a significant difference in the rates of EVR between subjects infected with group A and B isolates: EVR was achieved in 19 of 28 (68%) patients with group A infection, compared to 17 of 40 (43%) with group B infection ($P < 0.05$). The final outcome also differed significantly between subjects infected with group A and B isolates: SVR was achieved in 18 of 28 (64%) patients with group A infection, compared to 15 of 40 (38%) with group B infection ($P < 0.05$).

Polymorphisms in Core Amino Acids 70/91 and in the HCV NS3 Secondary Structure

The wild-type core sequence (Arg70, Leu91) has been associated with SVR in Peg-IFN/RBV combination therapy, while the non-double wild-type containing one or two substitutions at positions 70 and/or 91 was associated with non-SVR [Akuta et al., 2007]. Therefore, we examined substitutions at positions 70 and 91 in the HCV core region in pre-treatment serum samples of 44 cases that were available for testing. The double wild-type 70/91 sequence was found in 22 of the 44 cases (50%), of which 12 were SVR and 10 were non-SVR. Combination analysis of polymorphisms of the HCV core 70/91 positions and the NS3 amino-terminal region showed that 10 (83%) of the 12 SVR cases and only 3 (30%) of the 10 non-SVR cases with the double wild-type core had a group A polymorphism in HCV NS3 (Table IV). Thus, combination analysis of the core and NS3 regions may improve prediction of the outcome of Peg-IFN/RBV therapy.

TABLE II. Characteristics of Adherent Patients Infected With HCV Group A and B Isolates

	Group A (n = 28)	Group B (n = 40)	*P*
Age (years)	55.5 ± 9.5	55.5 ± 8.9	NS[a]
Sex (men/women)	18/10	21/19	NS[b]
Pre-treatment HCV RNA (KIU/ml)	1,635 ± 930	2,087 ± 1,422	NS[a]
Alanine aminotransferase level (U/L)	80 ± 62	71 ± 47	NS[a]
Stage of liver fibrosis			
F1 or F2/F3 or F4	19/9	28/12	NS[b]
Drug adherence dosage (%)			
Pegylated interferon	97.7 ± 5.2	95.2 ± 7.3	NS[a]
Ribavirin	96.8 ± 6.4	95.3 ± 7.7	NS[a]

NS, not significant.
[a]*t*-test.
[b]χ^2 test.

Re-Evaluation of Pre-Treatment HCV Viremia Status Using Real-Time PCR

Since the viral titer before treatment is a major predictive marker of the outcome of Peg-IFN/RBV therapy, we re-evaluated the pre-treatment viral titers more precisely using preserved serum samples taken within 1 month before treatment, using a real-time PCR assay. The pre-treatment viral titers did not differ significantly between sera with group A and B isolates (5.98 ± 0.94 vs. 6.25 ± 0.62 logIU/ml) (Table V). The secondary structure polymorphisms of HCV NS3 were independent of the pre-treatment viral titers.

DISCUSSION

Antiviral therapy with Peg-IFN/RBV for 48 weeks fails to eradicate HCV in about half of patients infected with a high titer of HCV genotype 1b, and the severe adverse events and high costs associated with this therapy require outcome prediction to allow targeted treatment for chronic hepatitis C. The pre-treatment viral titer, viral factors that influence the virological response to IFN-based anti-HCV therapy have been widely investigated. Viral kinetics showing prompt seronegativity after the start of treatment is a critical factor for achieving SVR, and thus the possible correlation between an early virological response and genetic sequence variation of the HCV has been studied. In particular, amino acid substitutions in the HCV core region at positions 70 and 91 or multiple mutations detected in the IRRDR of the HCV NS5A region are useful markers for predicting EVR and subsequent SVR.

TABLE III. Virological Responses in Subjects With Different Polymorphisms in the Secondary Structure of HCV NS3

	EVR*	ETR**	SVR*
Group A (n = 28)	19 (68%)	23 (82%)	18 (64%)
Group B (n = 40)	17 (43%)	25 (63%)	15 (38%)

EVR: early virological response at 12 weeks after the start of treatment.
ETR: virological response at the end of treatment.
SVR: sustained virological response 24 weeks after completion of treatment.
*$P < 0.05$.
**$P = 0.08$; χ^2 test.

To date, the influence of several single amino acid substitutions and accumulation of these changes in the viral genome on the effect of IFN-based anti-HCV therapy has been examined. Since interactions between host and viral proteins in infected cells may influence the therapeutic effect of an antiviral agent, we focused on the association of structural polymorphism of a viral protein with the effect of Peg-IFN/RBV combination therapy in this study. Our results suggest that polymorphism analysis of secondary structure deduced from sequence variations in the HCV NS3 amino-terminal region can be used to predict viral responses to this therapy.

Amino acid sequences of the HCV NS3 amino-terminal region, which encodes a serine protease, vary greatly among HCV isolates. Interactions between HCV NS3 and host proteins may influence both oncogenesis and immunity, and thus elucidation of the biological significance of these interactions could result in a new prognostic marker for HCC or a predictive marker for anti-HCV therapy. First, HCV NS3 interacts with the p53 tumor suppressor to suppress p53-dependent apoptosis or p21 transcriptional activity [Ishido and Hotta, 1998; Kwun et al., 2001; Deng et al., 2006]. Transfection of a plasmid expressing the amino-terminal portion of HCV NS3 induces cell transformation in vitro, and transplanted cells proliferate with sarcoma-like features in vivo [Sakamuro et al., 1995]. These findings suggest that NS3 may be involved in the oncogenic pathway in HCV infection. We have shown that the secondary structure of the 120-residue amino-terminal region of NS3 (1,027–1,146) is classifiable into two major groups: A and B. This region encodes a serine protease and also includes p53-binding sites. Our

TABLE IV. Treatment Outcome of Cases With a Double Wild-Type Core Region and Different HCV NS3 Structural Polymorphism

	Group A (%)	Group B (%)	*P*
SVR (n = 12)	10 (83)	2 (17)	0.02[a]
Non-SVR (n = 10)	3 (30)	7 (70)	

SVR, sustained virological response.
[a]χ^2 test.

TABLE V. Pre-Treatment HCV RNA Levels Measured by Real-Time PCR for Subjects With Different HCV NS3 Structural Polymorphism

	Group A	Group B	*P*
SVR (n = 33)	5.78 ± 1.05	6.13 ± 0.71	NS[a]
Non-SVR (n = 35)	6.33 ± 0.59	6.32 ± 0.55	NS[a]
Total (n = 68)	5.98 ± 0.94	6.25 ± 0.62	NS[a]

SVR, sustained virological response. NS, not significant.
[a]*t* test.

previous cross-sectional studies revealed that the prevalence of group B infection is significantly higher in HCC cases than in non-HCC cases [Ogata et al., 2003], and that the group B infection is an independent risk factor for development of HCC in patients with chronic HCV infection [Nishise et al., 2007]. Second, NS3 interacts with host proteins associated with IFN signaling and thus influences cellular immunity. Since the serine protease encoded by the amino-terminal region of NS3 inhibits the IFN-signaling pathway, polymorphism of this region is likely to influence the effect of Peg-IFN/RBV combination therapy.

Several factors associated with the virological response to this therapy are well known, with adherence to both IFN and RBV strongly influencing outcome [Pearlman, 2004; Arase et al., 2005; Yamada et al., 2008]. In this study, we analyzed 75 cases in which >80% of the scheduled dosage of both drugs was administered. Of these cases, 28 (37%) and 40 (53%) were infected with group A and B isolates, respectively, which were similar rates to those for the 139 cases in the overall study. Age, gender, viral load before treatment, ALT level, proportion of fibrosis stage and adherence to Peg-IFN and RBV did not differ between the group A and B cases. However, the frequencies of SVR and EVR were significantly higher in group A, and those for non-EVR and non-SVR were significantly higher in group B. The results suggest that infection with the group B isolate, which correlates with a higher rate of HCC, is resistant to Peg-IFN/RBV therapy. The pre-treatment viremia status in the 68 cases with group A or B isolates showed no significant differences between the two groups of patients. Therefore, these results suggest that the secondary structure of the HCV NS3 amino-terminal region may be useful for prediction of the outcome of Peg-IFN/RBV combination therapy. In this initial study setting, the relationship of these polymorphisms to the frequency of rapid viral response at 4 weeks after the start of treatment was not evaluated. It will be important to assess this relationship in a future study.

The polymorphism in HCV core region (Arg70/Leu91) is a useful predictive marker for virological responses in Peg-IFN/RBV therapy [Akuta et al., 2007]. Interestingly, a combined analysis of polymorphisms of the core region (which encodes a structural protein) and HCV NS3 (a nonstructural protein) improved the prediction rate. Therefore, analysis of NS3 polymorphism in combination with the core structural polymorphism appears to improve prediction of the outcome of Peg-IFN/RBV therapy. A larger, multi-center prospective study would be necessary to validate the present results. In conclusion, the results of this study suggest that secondary structure polymorphism in the amino-terminal region of HCV NS3 is a useful predictive marker of the effect of Peg-IFN/RBV combination therapy for chronic hepatitis C. Although the present findings are clinically important, and will be helpful for predicting the outcome of Peg-IFN/RBV therapy, further in vitro studies will be needed to elucidate the molecular mechanism underlying the association of HCV NS3polymorphisms with clinical outcome.

REFERENCES

Akuta N, Suzuki F, Sezaki H, Suzuki Y, Hosaka T, Someya T, Kobayashi M, Saitoh S, Watahiki S, Sato J, Kobayashi M, Arase Y, Ikeda K, Kumada H. 2006. Predictive factors of virological non-response to interferon-ribavirin combination therapy for patients infected with hepatitis C virus of genotype 1b and high viral load. J Med Virol 78:83–90.

Akuta N, Suzuki F, Kawamura Y, Yatsuji H, Sezaki H, Suzuki Y, Hosaka T, Kobayashi M, Kobayashi M, Arase Y, Ikeda K, Kumada H. 2007. Predictive factors of early and sustained responses to peginterferon plus ribavirin combination therapy in Japanese patients infected with hepatitis C virus genotype 1b: Amino acid substitutions in the core region and low-density lipoprotein cholesterol levels. J Hepatol 46:403–410.

Arase Y, Ikeda K, Tsubota A, Suzuki F, Suzuki Y, Saitoh S, Kobayashi M, Akuta N, Someya T, Hosaka T, Sezaki H, Kobayashi M, Kumada H. 2005. Significance of serum ribavirin concentration in combination therapy of interferon and ribavirin for chronic hepatitis C. Intervirology 48:138–144.

Bruno S, Cammà C, Di Marco V, Rumi M, Vinci M, Camozzi M, Rebucci C, Di Bona D, Colombo M, Craxì A, Mondelli MU, Pinzello G. 2004. Peginterferon alfa-2b plus ribavirin for naïve patients with genotype 1 chronic hepatitis C: A randomized controlled trial. J Hepatol 41:474–481.

Deng L, Nagano-Fujii M, Tanaka M, Nomura-Takigawa Y, Ikeda M, Kato N, Sada K, Hotta H. 2006. NS3 protein of hepatitis C virus associated with the tumor suppressor p53 and inhibits its function in an NS3 sequence-dependent manner. J Gen Virol 87:1703–1713.

El-Shamy A, Sasayama M, Nagano-Fujii M, Sasase N, Imoto S, Kim SR, Hotta H. 2007. Prediction of efficient virological response to pegylated interferon/ribavirin combination therapy by NS5A sequences of hepatitis C virus and anti-NS5A antibodies in pre-treatment sera. Microbiol Immunol 51:471–482.

El-Shamy A, Nagano-Fujii M, Sasase N, Imoto S, Kim SR, Hotta H. 2008. Sequence variation in hepatitis C virus nonstructural protein 5A predicts clinical outcome of pegylated interferon/ribavirin combination therapy. Hepatology 48:38–47.

Enomoto N, Sakuma I, Asahina Y, Kurosaki M, Murakami T, Yamamoto C, Ogura Y, Izumi N, Marumo F, Sato C. 1996. Mutations in the nonstructural protein 5A gene and response to interferon in patients with chronic hepatitis C virus 1b infection. N Engl J Med 334:77–81.

Evans JD, Seeger C. 2006. Cardif: A protein central to innate immunity is inactivated by the HCV NS3 serine protease. Hepatology 43:615–617.

Foy E, Li K, Wang C, Sumpter R, Jr., Ikeda M, Lemon SM, Gale M, Jr. 2003. Regulation of interferon regulatory factor-3 by the hepatitis C virus serine protease. Science 300:1145–1148.

Gale MJ, Jr., Korth MJ, Tang NM, Tan SL, Hopkins DA, Dever TE, Polyak SJ, Gretch DR, Katze MG. 1997. Evidence that hepatitis C virus resistance to interferon is mediated through repression of the PKR protein kinase by the nonstructural 5A protein. Virology 230:217–227.

Gale MJ, Jr., Korth MJ, Katze MG. 1998. Repression of the PKR protein kinase by the hepatitis C virus NS5A protein: A potential mechanism of interferon resistance. Clin Diagn Virol 10:157–162.

Garnier J, Osguthorfe DJ, Robson B. 1978. Analysis of the accuracy and implications of simple methods for predicting the secondary structure of globular proteins. J Mol Biol 120:97–120.

Grandvaux N, Servant MJ, tenOever B, Sen GC, Balachandran S, Barber GN, Lin R, Hiscott J. 2002. Transcriptional profiling of interferon regulatory factor 3 target genes: Direct involvement in the regulation of interferon-stimulated genes. J Virol 76:5532–5539.

Hadziyannis SJ, Sette H, Jr., Morgan TR, Balan V, Diago M, Marcellin P, Ramadori G, Bodenheimer H, Jr., Bernstein D, Rizzetto M, Zeuzem S, Pockros PJ, Lin A, Ackrill AM. 2004. Peginterferon-alpha2a and ribavirin combination therapy in chronic hepatitis C: A randomized study of treatment duration and ribavirin dose. Ann Intern Med 140:346–355.

Hiramatsu N, Kurashige N, Oze T, Takehara T, Tamura S, Kasahara A, Oshita M, Katayama K, Yoshihara H, Imai Y, Kato M, Kawata S, Tsubouchi H, Kumada H, Okanoue T, Kakumu S, Hayashi N. 2008. Early decline of hemoglobin can predict progression of hemolytic anemia during pegylated interferon and ribavirin combination therapy in patients with chronic hepatitis C. Hepatol Res 38:52–59.

Ishido S, Hotta H. 1998. Complex formation of the nonstructural protein 3 of hepatitis C virus with the p53 tumor suppressor. FEBS Lett 438:258–262.

Kwun HJ, Jung EY, Ahn JY, Lee MN, Jang KL. 2001. p53-dependent transcriptional repression of p21(waf1) by hepatitis C virus NS3. J Gen Virol 82:2235–2241.

Manns MP, McHutchison JG, Gordon SC, Rustgi VK, Shiffman M, Reindollar R, Goodman ZD, Koury K, Ling M, Albrecht JK. 2001. Peginterferon alfa-2b plus ribavirin compared with interferon alfa-2b plus ribavirin for initial treatment of chronic hepatitis C: A randomized trial. Lancet 358:958–965.

Meylan E, Curran J, Hofmann K, Moradpour D, Binder M, Bartenschlager R, Tschopp J. 2005. Cardif is an adaptor protein in the RIG-I antiviral pathway and is targeted by hepatitis C virus. Nature 437:1167–1172.

Murphy MD, Rosen HR, Marousek GI, Chou S. 2002. Analysis of sequence configurations of the ISDR, PKR-binding domain, and V3 region as predictors of response to induction interferon-alpha and ribavirin therapy in chronic hepatitis C infection. Dig Dis Sci 47:1195–1205.

Nakaya T, Sato M, Hata N, Asagiri M, Suemori H, Noguchi S, Tanaka N, Taniguchi T. 2001. Gene induction pathways mediated by distinct IRFs during viral infection. Biochem Biophys Res Commun 283:1150–1156.

Nishise Y, Saito T, Sugahara K, Ito JI, Saito K, Togashi H, Nagano-Fujii M, Hotta H, Kawata S. 2007. Risk of hepatocellular carcinoma and secondary structure of hepatitis C virus (HCV) NS3 protein amino-terminus, in patients infected with HCV subtype 1b. J Infect Dis 196:1006–1009.

Nousbaum J, Polyak SJ, Ray SC, Sullivan DG, Larson AM, Carithers RL, Jr., Gretch DR. 2000. Prospective characterization of full-length hepatitis C virus NS5A quasispecies during induction and combination antiviral therapy. J Virol 74:9028–9038.

Ogata S, Ku Y, Yoon S, Makino S, Nagano-Fujii M, Hotta H. 2002a. Correlation between secondary structure of an amino-terminal portion of the nonstructural protein 3 (NS3) of hepatitis C virus and development of hepatocellular carcinoma. Microbiol Immunol 46:549–554.

Ogata S, Nagano-Fujii M, Ku Y, Yoon S, Hotta H. 2002b. Comparative sequence analysis of the core protein and its frameshift product, the F protein, of hepatitis C virus subtype 1b strains obtained from patients with and without hepatocellular carcinoma. J Clin Microbiol 40:3625–3630.

Ogata S, Florese RH, Nagano-Fujii M, Hidajat R, Deng L, Ku Y, Yoon S, Saito T, Kawata S, Hotta H. 2003. Identification of hepatitis C virus (HCV) subtype 1b strains that are highly, or only weakly, associated with hepatocellular carcinoma on the basis of the secondary structure of an amino-terminal portion of the HCV NS3 protein. J Clin Microbiol 41:2835–2841.

Pearlman BL. 2004. Hepatitis C treatment update. Am J Med 117:344–352.

Puig-Basagoiti F, Forns X, Furcić I, Ampurdanés S, Giménez-Barcons M, Franco S, Sánchez-Tapias JM, Saiz JC. 2005. Dynamics of hepatitis C virus NS5A quasispecies during interferon and ribavirin therapy in responder and non-responder patients with genotype 1b chronic hepatitis C. J Gen Virol 86:1067–1075.

Sakamuro D, Furukawa T, Takegami T. 1995. Hepatitis C virus nonstructural protein NS3 transforms NIH 3T3 cells. J Virol 69: 3893–3896.

Sarrazin C, Herrmann E, Bruch K, Zeuzem S. 2002. Hepatitis C virus nonstructural 5A protein and interferon resistance: A new model for testing the reliability of mutational analyses. J Virol 76:11079–11090.

Yamada K, Mori A, Seki M, Kimura J, Yuasa S, Matsuura Y, Miyamura T. 1998. Critical point mutations for hepatitis C virus NS3 proteinase. Virology 246:104–112.

Yamada G, Iino S, Okuno T, Omata M, Kiyosawa K, Kumada H, Hayashi N, Sakai T. 2008. Virological response in patients with hepatitis C virus genotype 1b and a high viral load: Impact of peginterferon-alpha-2a plus ribavirin dose reductions and host-related factors. Clin Drug Investig 28:9–16.